Available online at www.sciencedirect.com

SCIENCE DIRECT

Biochimica et Biophysica Acta 1708 (2005) 283 – 310

BIOCHIMICA ET BIOPHYSICA ACTA
BBA

http://www.elsevier.com/locate/bba

Review

Modelling of the electron transfer reactions in Photosystem I by electron tunnelling theory: The phylloquinones bound to the PsaA and the PsaB reaction centre subunits of PS I are almost isoenergetic to the iron–sulfur cluster F_X

Stefano Santabarbara[a,b,*], Peter Heathcote[a], Michael C.W. Evans[b]

[a]*School of Biological Sciences, Queen Mary, University of London, Mile End Road, London E1 4NS, UK*
[b]*Department of Biology, University College London, Gower Street, London WC1E, 6BT, UK*

Received 27 October 2004; received in revised form 12 April 2005; accepted 3 May 2005
Available online 31 May 2005

Abstract

Photosystem I is a large macromolecular complex located in the thylakoid membranes of chloroplasts and in cyanobacteria that catalyses the light driven reduction of ferredoxin and oxidation of plastocyanin. Due to the very negative redox potential of the primary electron transfer cofactors accepting electrons, direct estimation by redox titration of the energetics of the system is hampered. However, the rates of electron transfer reactions are related to the thermodynamic properties of the system. Hence, several spectroscopic and biochemical techniques have been employed, in combination with the classical Marcus theory for electron transfer tunnelling, in order to access these parameters. Nevertheless, the values which have been presented are very variable. In particular, for the case of the tightly bound phylloquinone molecule A_1, the values of the redox potentials reported in the literature vary over a range of about 350 mV. Previous models of Photosystem I have assumed a unidirectional electron transfer model. In the present study, experimental evidence obtained by means of time resolved absorption, photovoltage, and electron paramagnetic resonance measurements are reviewed and analysed in terms of a bi-directional kinetic model for electron transfer reactions. This model takes into consideration the thermodynamic equilibrium between the iron–sulfur centre F_X and the phylloquinone bound to either the PsaA (A_{1A}) or the PsaB (A_{1B}) subunit of the reaction centre and the equilibrium between the iron–sulfur centres F_A and F_B. The experimentally determined decay lifetimes in the range of sub-picosecond to the microsecond time domains can be satisfactorily simulated, taking into consideration the edge-to-edge distances between redox cofactors and driving forces reported in the literature. The only exception to this general behaviour is the case of phylloquinone (A_1) reoxidation. In order to describe the reported rates of the biphasic decay, of about 20 and 200 ns, associated with this electron transfer step, the redox potentials of the quinones are estimated to be almost isoenergetic with that of the iron sulfur centre F_X. A driving force in the range of 5 to 15 meV is estimated for these reactions, being slightly exergonic in the case of the A_{1B} quinone and slightly endergonic, in the case of the A_{1A} quinone. The simulation presented in this analysis not only describes the kinetic data obtained for the wild type samples at room temperature and is consistent with estimates of activation energy by the analysis of temperature dependence, but can also explain the effect of the mutations around the PsaB quinone binding pocket. A model of the overall energetics of the system is derived, which suggests that the only substantially irreversible electron transfer reactions are the reoxidation of A_0 on both electron transfer branches and the reduction of F_A by F_X.

Keywords: Photosystem I; Electron transfer; Phylloquione A_1; Iron–sulphur centre (F_X, F_A, F_B); Redox potential

1. Introduction

Photosystem I (PS I) is a large macromolecular complex, located in the thylakoid membranes of oxygenic

* Corresponding author. School of Biological Sciences, Queen Mary, University of London, London, E1 4NS, UK. Tel.: +44 20 7882 4124; fax: +44 20 8983 0973.
E-mail address: s.santabarbara@qmul.ac.uk (S. Santabarbara).

0005-2728/$ - see front matter © 2005 Elsevier B.V. All rights reserved.
doi:10.1016/j.bbabio.2005.05.001

photosynthetic organisms, which catalyses the light-driven oxidation of the soluble carrier plastocyanin on the stromal side of the membrane and the reduction of ferredoxin on the lumenal side of the membrane. The core of PS I is composed of 12 to 13 different polypeptides, depending on species, and binds a large number of cofactors, most of which are Chl *a* (~100) and β-carotene (~30), which act as inner antenna, but are not involved in electron transfer reactions. The majority of the electron transfer events are mediated by redox cofactors bound to the PsaA–PsaB subunits heterodimer [1–3]. The electron transfer reactions are initiated by the absorption of a photon, which drives the primary charge separation event at the level of the primary donor, P_{700}. [4–6]. The first spectroscopically resolved electron acceptor named A_0 is again a Chl *a* molecule [7–12] and is generally thought to be reduced on a very short time scale, of less then 10 ps [9,13–19]. The electrons are then transferred to a tightly bound phylloquinone molecule [7,8,20–22], A_1, in about 20–40 ps [9,14,16,18,19,23]. This, in turn, reduces the first of a series of [4Fe–4S] iron–sulfur clusters [24–33], F_X, with a markedly biphasic kinetic, with characteristic lifetimes of about ~20 ns and ~200 ns [34–39]. The electron transfer reactions then proceed to reduce the iron–sulfur centres [24,25,27,28,30,40,41] F_A and F_B, which are bound to the PsaC subunits [42–44], and finally reduce a diffusible electron transfer carrier, which is usually ferredoxin (Fd) [45].

The X-ray crystallographic structure of PS I has been solved in both a cyanobacterial [1–3] and a higher plant system [46]. Despite the differences in the antenna arrangement and the presence of different species-specific protein subunits, the arrangement of the redox cofactors appears highly conserved in the two X-ray structures. At the present level of resolution of the *Synechoccoccus elongatus* PS I reaction centre structure (2.5 Å), all the electron transfer cofactors, previously identified by spectroscopic investigations, can be assigned together with the protein surrounding [3]. The structure clearly shows how the electron transfer cofactors are arranged in a highly symmetrical manner with respect to the axis perpendicular to the membrane plane. The only apparent asymmetry in the whole electron transfer chain appears at the level of the primary donor which is a heterodimer of a Chl *a* and a Chl *a*′ epimer [3]. For the rest, the protein scaffold and the distance between the redox centres bound either to the PsaA or the PsaB subunits appear similar, suggesting that both electron transfer branches could be active in the electron transfer reactions, which is at odds with what is observed for the reaction centre of the purple bacteria. An obvious difference between the two reaction centres is that PS I and, generally, type I reaction centres (which are characterised by Fe–S clusters as terminal electron acceptors) do not operate a two-electron gate mechanism, in contrast to type II reaction centres.

However, at present, there is still a lack of general agreement regarding the directionality of electron transfer within the PS I reaction centre [19,36,37,47–52]. Most of the observations which have led to the suggestion of a bi-directional electron transfer events were obtained by the analysis of the reoxidation reactions of the A_1 phylloquinone, in terms of their temperature dependence [38,53] and the effect of site-directed mutation [37]. It is generally accepted that the slow phase of A_1 reoxidation is associated with the PsaA-bound phylloquinone (A_{1A}), as observed by both transient electron paramagnetic resonance (EPR) [21,33,54–58] and optical spectroscopy [19,35–37,53,59]. The centre of the controversy concerns whether and to what extent the PsaB-bound chlorophylls and quinone (A_{1B}) take part in the electron transfer process [37,48,49,51,52]. In order to explain the marked biphasic kinetics of reoxidation of the A_1 semi-phylloquinone, several hypotheses have been put forward. The original interpretation that the fast ~20 ns reoxidation phase might have derived from a purification artefact [34] was abandoned after the observation that A_1 reoxidation is biphasic in intact green algae cells [36,37]. Setif and Brettel [19,53,59] had suggested that the observed biphasic kinetic was explainable in term of a small driving force for the electron transfer reaction between A_1 and F_X. The fast phase in this hypothesis frame, which is often referred to as the "quasi-equilibrium model", would essentially reflect the rate of F_X reoxidation, while the slow phase would mainly reflect the actual A_1 quinone reoxidation. Evidence for this model comes from the observed temperature dependence of A_1 reoxidation reaction, for which a rather large activation energy, determined from the classical Arrhenius relation, of about 100–200 meV has been estimated [53]. However, in a more recent reinvestigation, the fast ~20 ns phase has been resolved and has been shown to possess a much lower activation energy of about 15 meV [38]. The hypothesis that the fast reoxidation rate is associated with the A_{1B} quinone reoxidation has been put forward by Joliot and coworkers [36,37] based on the observation that mutation in the PsaA quinone binding site affects substantially only the ~200 ns reoxidation rate, while symmetrical mutation in the PsaB quinone binding site essentially affects only the ~20 ns reoxidation rate [37].

Mutations at the level of the primary acceptor A_0 have been shown to affect the electron spin polarised (ESP) signal associated with secondary radical couple [$P_{700}^{+}A_1^{-}$] [51,52,60]. While there is a broad consensus as regards the effect of substitution of the axial ligand to the A_0 on the PsaA subunit, leading to the lengthening of the [$P_{700}^{+}A_0^{-}$] primary radical pair lifetime and hence loss of spin coherence in the successive electron transfer step, contrasting reports have been presented related to the effect of A_0 axial ligand mutagenesis on the PsaB subunit of the reaction centre [51,52,60,61]. When the natural methionine ligand, which provides a weak axial ligand via

the thio-alcohol side chain, is substituted with an alanine (which is unlikely to provide any axial donor, unless by a water bridge), no appreciable change in the spin polarised radical pair has been reported [52,60]. In contrast, the symmetric mutation on the PsaA subunit has a more dramatic effect, therefore questioning the bi-directional model for PS I electron transfer [52,60]. However, the substitution of the methionine axial ligand with a histidine (which may act as a stronger donor) on both the reaction centre subunits has been demonstrated to affect the forward and the recombination kinetic [51,61]. The decay of the spin-polarised electron spin echo signal associated with the $[P_{700}^{+}A_{1}^{-}]$ radical pair reflects forward electron transfer from the A_{1A} phylloquinone at room temperature [50,58,62]. Substitution of the natural methionine ligand with an histidine on the PsaA subunit (mutant PsaA-M684H) essentially suppressed the signal [51]. The effect of the symmetrical mutation on the PsaB subunit cannot be monitored by time-resolved EPR due to limited time resolution. However, the decay of the $[P_{700}^{+}A_{1}^{-}]$ radical pair at 100 K has been shown to be markedly biphasic when the iron–sulfur acceptor F_X is reduced and described by two lifetime components of about ~2–5 μs and ~15–20 μs [50,51,61]. In these conditions, forward electron transfer is blocked, and charge recombination may occur [19,53,63–65], although the decay rate reflects a mixture of charge recombination lifetime and loss of spin correlation. It has been shown that in the PsaA-M664H mutant, the 15–20 μs phase of the $[P_{700}^{+}A_{1}^{-}]$ radical pair decay at 100 K is selectively suppressed [51]. The 2–5 μs phase is selectively suppressed in PsaB-M664H [51]. The most straightforward explanation for these results is that the two phases of $[P_{700}^{+}A_{1}^{-}]$ decay are correlated with the charge recombination reaction of P_{700}^{+} with the one or the other of the two phylloquinones bound to each reaction centre subunit [50,51]. Furthermore, the analysis of the "out-of-phase"-ESEEM in the site-directed A_0 mutants demonstrated the presence of two different $[P_{700}^{+}A_{1}^{-}]$ radical pairs, populated either on the PsaA or the PsaB branch of the reaction centre [61]. The distances between the partners in the radical pairs (A_{1A}^{-} and P_{700}^{+}, and A_{1B}^{-} and P_{700}^{+}) estimated from the evaluation of the spin–spin interaction energies [61] are in agreement with the crystallographic structure [3], when the asymmetry of spin distribution of P_{700}^{+} is taken into consideration [66–71].

Light could be shed on the controversy regarding the directionality of ET in Photosystem I, if the redox potentials of the cofactors were known. Unfortunately, the acceptor side of PS I operates at rather negative redox potentials; therefore, a direct titration of the redox centres has not been possible, except for the electron donor P_{700} and the terminal iron–sulfur clusters F_X, F_A, and F_B [24,25,28,40,72–79]. However, indirect estimation of the midpoint potential for almost all the redox centres has been obtained by a variety of spectroscopic investigations. This approach has not yielded a consensus regarding the potential of A_1 as the estimates produce values in the −(820–530) mV range [80,81,82]. In the following study, we present an attempt to model the electron transfer reactions in PS I based on the electron tunnelling theory for biological samples [83–85], using a bi-directional kinetic model, which includes thermodynamic equilibrium between all the electron transfer steps, in order to try to abstract information about the redox potential of electron transfer cofactors which are not directly titratable. For clarity, the reactions happening on different time scales are discussed in separate sections. Experimental observations obtained by means of time resolved absorption, photovoltage, and electron paramagnetic resonance measurements are considered, and it will be shown that they can be reasonably reconciled within the model presented in this paper. Particular attention is paid to the rate of reoxidation of the A_1 phylloquinones, since most of the information which indicates that cofactors bound to both the reaction centre subunits are active in PS I electron transfer were obtained through monitoring the direct or indirect effects on this reaction.

2. Electron transfer tunnelling theory applied to Photosystem I

2.1. Overview on electron transfer tunnelling in biological samples

The electron transfer rate constant (k_{et}) can be calculated according to the Marcus formalism for electron tunnelling [84,86–88]:

$$k_{et} = \frac{2\cdot\pi\cdot |V|^2}{\sqrt{4\cdot\pi\cdot\lambda_t\cdot k_B\cdot T}}\cdot e^{-\frac{(\lambda_t+\Delta G^0)^2}{4\cdot\lambda_t\cdot k_B\cdot T}} \quad (1)$$

where V is the electronic coupling matrix element, which is dependent on the distance between the reactants; ΔG_0 is the Gibbs free energy; k_B is the Boltzmann constant; T is the temperature of the lattice; and λ_t is the total reorganisation energy of the reaction and can be described as the sum of the reorganisation energy of the medium (λ_{out}) and the reactant (λ_{in}). The

reorganisation energy represents the amount of energy which is needed to perturb the nuclear configuration of the donor molecules, so that it reaches the intermediate activated state and can proceed to the final equilibrium configuration after the electron transfer reaction has taken place. It is generally related to the small rearrangement of bond lengths and dipole distribution, either of the electron transfer molecules or of the surrounding medium. The reorganisation energy (λ) and the driving force for the reaction (ΔG^0) determine the activation energy (ΔG^*), which can be written in terms of the Marcus theory as [84,86–88]:

$$\Delta G^* = \frac{(\lambda + \Delta G^0)^2}{4 \cdot \lambda} \tag{2}$$

It is clear from the form of Eqs. (1) and (2) that the maximum rate of electron transfer is achieved when $\Delta G^0 = -\lambda$ and that, in that case, the reaction will be activationless.

Eq. (1) can be extended to take into account coupling of the electron transfer reaction with a main single molecular vibrational mode. The quantum-mechanical expression which describes the electron transfer is given by [89]:

$$k_{et} = \frac{2 \cdot \pi \cdot |V|^2}{\hbar \cdot \omega} \cdot \exp\left(-S \cdot (2z+1)\right) \left(\frac{z+1}{z}\right)^{p/2} \cdot I_p\left(2 \cdot S \cdot \sqrt{z \cdot (z+1)}\right) \tag{3}$$

where S, p, and z are defined as:

$$S = \frac{\lambda_t}{\hbar \cdot \omega}; \quad p = \frac{-\Delta G}{\hbar \cdot \omega}; z = (e^{\frac{\hbar\omega}{k_B T}} - 1)^{-1}; \text{ and}$$
$$I_p(\xi) = \sum_{k=0}^{\infty} \frac{(\xi/2)^{p+2k}}{k! \Gamma(p+k+1)} \tag{4}$$

$I_p(\xi)$ is the Bessel Function of order p, as extended to non-integer values for p. All the other symbols have the same meaning as in Eq. (1), and ω is the angular frequency of the main lattice (protein) vibration.

It has been demonstrated that the electron transfer in a large range of electron transfer proteins can described by a simplified form of Eq. (4) [85,89–91]:

$$\log_{10} k_{et} = 13 - (1.2 - 0.8 \cdot \rho) \cdot (X_{AB} - 3.6) - 0.22 \frac{(\Delta G^0 + \lambda_t)^2}{\lambda \cdot \hbar \cdot \omega \cdot \mathrm{Coth}\left(\frac{\hbar \cdot \omega}{2 \cdot k_B \cdot T}\right)} \tag{5}$$

where ρ is a parameter defined as the protein packing density and is correlated to the energetic barrier the electrons have to travel in the tunnelling process; and X_{AB} is the edge-to-edge distance between the cofactors bound to the protein. At room temperature, Eq. (3) can be further simplified yielding the following relationship [85,90,91]:

$$\log_{10} k_{et}^{RT} = 13 - (1.2 - 0.8 \cdot \rho) \cdot (X_{AB} - 3.6) - 3.1 \frac{(\Delta G^0 + \lambda_t)^2}{\lambda_t} \tag{6}$$

Since most of the measurements which we have attempted to describe in this manuscript have been performed at room temperature (300 K), Eq. (5) has been generally used to derive the forward electron transfer rate (unless otherwise specified), and the equilibrium constant has then been estimated from the Boltzmann distribution.

2.2. Bi-directional kinetic model of PS I electron transfer reactions

A kinetic model which takes into account electron transfer on both the PsaA and the PsaB subunits of the PS I reaction centre, and which takes into account the population equilibrium in between each of the electron transfer steps, has been

developed. The dynamics of the population of each electron transfer chain intermediate can be evaluated by the numerical solution of a system of (coupled) differential Eq. (7):

$$\begin{cases}
\frac{\delta}{\delta t}[\mathrm{Ant^*P_{700}}](t) = -k_0[\mathrm{Ant^*P_{700}}](t) + k_{-0}\left[\mathrm{P^*_{700}P_{700}}\right](t) \\
\frac{\delta}{\delta t}\left[\mathrm{P^*_{700}P_{700}}\right](t) = -(k_1 + k_{10} + k_{-0})\left[\mathrm{P^*_{700}P_{700}}\right](t) + k_0\left[\mathrm{P^*_{700}P_{700}}\right](t) + k_{-1}\left[\mathrm{P^+_{700}A^-_{0A}}\right](t) + k_{-10}\left[\mathrm{P^+_{700}A^-_{0B}}\right](t) \\
\frac{\delta}{\delta t}\left[\mathrm{P^+_{700}A^-_{0A}}\right](t) = -(k_2 + k_{-1})\left[\mathrm{P^+_{700}A^-_{0A}}\right](t) + k_1\left[\mathrm{P^*_{700}P_{700}}\right](t) + k_{-2}\left[\mathrm{P^+_{700}A^-_{1A}}\right](t) \\
\frac{\delta}{\delta t}\left[\mathrm{P^+_{700}A^-_{0B}}\right](t) = -(k_{20} + k_{-10})\left[\mathrm{P^+_{700}A^-_{0B}}\right](t) + k_{10}\left[\mathrm{P^*_{700}P_{700}}\right](t) + k_{-20}\left[\mathrm{P^+_{700}A^-_{1B}}\right](t) \\
\frac{\delta}{\delta t}\left[\mathrm{P^+_{700}A^-_{1A}}\right](t) = -(k_3 + k_{-2})\left[\mathrm{P^+_{700}A^-_{1A}}\right](t) + k_2\left[\mathrm{P^+_{700}A^-_{0A}}\right](t) + k_{-3}\left[\mathrm{P^+_{700}F^-_X}\right](t) \\
\frac{\delta}{\delta t}\left[\mathrm{P^+_{700}A^-_{1B}}\right](t) = -(k_{30} + k_{-20})\left[\mathrm{P^+_{700}A^-_{1B}}\right](t) + k_{20}\left[\mathrm{P^+_{700}A^-_{0B}}\right](t) + k_{-30}\left[\mathrm{P^+_{700}F^-_X}\right](t) \\
\frac{\delta}{\delta t}\left[\mathrm{P^+_{700}F^-_X}\right](t) = -(k_4 + k_{-3} + k_{-30})\left[\mathrm{P^+_{700}F^-_X}\right](t) + k_3\left[\mathrm{P^+_{700}A^-_{1A}}\right](t) + k_{30}\left[\mathrm{P^+_{700}A^-_{1B}}\right](t) + k_{-4}\left[\mathrm{P^+_{700}F^-_B}\right](t) \\
\frac{\delta}{\delta t}\left[\mathrm{P^+_{700}F^-_A}\right](t) = -(k_5 + k_{-4})\left[\mathrm{P^+_{700}F^-_A}\right](t) + k_4\left[\mathrm{P^+_{700}F^-_X}\right] + k_{-5}\left[\mathrm{P^+_{700}F^-_B}\right](t) \\
\frac{\delta}{\delta t}\left[\mathrm{P^+_{700}F^-_B}\right](t) = -(k_6 + k_{-5})\left[\mathrm{P^+_{700}F^-_B}\right](t) + k_5\left[\mathrm{P^+_{700}F^-_A}\right](t)
\end{cases} \tag{7}$$

The eigenvalues of the system of differential equations represent the measured lifetime components, and the eigenvectors have been estimated assuming that the initial excited state population entirely resides in the antenna of Photosystem I. Two parameters were considered in the estimate of the average lifetime of the distribution, the first moment of the decay, which is described by the equation:

$$\bar{\tau} = \int_0^\infty t \cdot f(t)\mathrm{d}t \tag{8}$$

and the weighted average lifetime

$$\tau_{\mathrm{av}} = \sum_{i=1}^{n} A_{\mathrm{i}}\tau_{\mathrm{i}} \tag{9}$$

where A_{i} and τ_{i} are the eigenvector and eigenvalues solutions of the system of differential equation and reflect the pre-exponential and characteristic lifetimes determined experimentally.

2.3. Estimation of electron transfer tunnelling parameters in PS I

2.3.1. Distances

The edge-to-edge distances have been taken from the deposited crystal structure of cyanobacterial Photosystem I refined at 2.5 Å resolution [3].

2.3.2. Protein density packing (ρ)

Ivashin and Larsson [92] have performed an analysis of the protein surrounding the quinone and iron–sulfur F_X region and reported no significant difference in the protein environment, although they did not explicitly report the calculated value for protein packaging or the dielectric constant of the medium in their study. In their analysis of electron tunnelling in redox active proteins, Page and coworkers [91] have explored the value of the protein density packing parameters in a variety of systems. They found that the value of ρ is widely distributed but has a mean value of about 0.75 in the electron transfer proteins investigated in their study. Therefore, we have used this value in the computation of the rate constants of electron transfer reactions in PS I.

2.3.3. Gibbs free energy

Due to the extremely low redox potentials of the electron transfer cofactors in Photosystem I, no direct redox titration has been presented in the literature, except for the electron donor P^+_{700} and the iron–sulfur clusters, $F_{X/A/B}$. Nonetheless, several estimates of the potentials have been indirectly obtained by a wide range of spectroscopic techniques, but are often controversial. The values reported in the literature are critically reviewed and discussed.

3. Electron transfer reaction in PS I

3.1. Electron transfer events in the femto- to picosecond time scale: charge separation and primary radical pairs

The reaction centre of PS I contains a large number of chlorophyll pigments, which function as a proximal antenna in addition to the primary donor P_{700} and the first spectroscopically resolved chlorin acceptor, A_0. Some of the antenna chlorophyll forms absorb at wavelengths longer than the reaction centre itself and are often referred as the "red forms" [97–106]. This is particularly the case in cyanobacteria, in which forms which are as red shifted as 50 nm compared with the RC proper have been reported [97,98,102,105,107–109]. On the other hand, in higher plant systems, most of the red absorbing forms are associated with the outer antenna complexes [104,110,111]. The interpretation of optical transients directly attributable to the primary charge separation reaction is often complicated as the very short lifetime of the primary radical pairs overlap with the evolution of the excited state populations in the antenna, because of uphill energy transfer from the 'red-absorbing' chlorophyll forms. In order to accommodate the results from sub-picosecond transient absorption and the kinetics of fluorescence decay, a model in which the primary photochemical events are considered to be transfer-to-trap limited has been proposed [18,102,107,112]. The primary charge separation is then estimated to take place with rates of about $k_{fc} \sim (1-10\ ps)^{-1}$. The secondary radical pair is then formed in tens of picoseconds [18,102,107,112–114].

A detailed attempt to describe the sub-picosecond evolution has not been pursued in the present study, as these transients are mainly related to excited state equilibration within the antenna, the antenna and the reaction centre proper, and equilibration within the reaction centre proper, although the transfer of the excited state from the antenna to the trap is formally considered for consistency with previous models reported in the literature. This is the subject of recent studies in which techniques, such as fluorescence up-conversion, synchronous streak-camera time resolved fluorescence, as well as multicolour pump-probe spectroscopy [11,14,16–18,102,107,113–136], have been employed and which have been recently reviewed [102,124].

Recently, Muller and coworkers [130] have reinvestigated the problem of charge separation in a Photosystem I preparation from the green alga *C. reinhardtii*. This organism has an antenna with is particularly poor in red chlorophyll forms and, therefore, is particularly suitable for optical investigations of the kinetics of primary charge separation due to the reduced interference of antenna excited state equilibration with the primary photochemical reactions. The authors reported the presence of at least four lifetime distributions, obtained by direct transformation of the time domain optical transient, centred at about ~800 fs, ~6 ps, ~20 ps, and ~40 ps, which might be taken into consideration in order to model the primary electron transfer reaction in PS I [130]. It should be kept in mind that none of the observed transients can be exhaustively interpreted as a rate constant, but rather reflect the result of the coupled electron transfer reaction rates, whether equilibration between the radical pair states is taken into account or not. On the other hand, some information can be directly abstracted from the inspection of the spectral dependence of the lifetime distributions. For example, the lifetime component in the 6–8 ps range could be attributed to the rise time of the primary radical pair state [130], based on the presence of an absorption band in the 740–760 nm region, which is a fingerprint of this species [9,137]. In order to correctly describe the optical transients in terms of species associated spectra (SAS), Muller et al. proposed that three radical pair states must be taken into consideration [130], and it was suggested that one of these radical pair states might involve the so-called accessory chlorophylls, labelled as ChlA2 and ChlB2 in the X-ray structure [3].

An examination of the SAS presented by these authors shows that the SAS associated with the second ('RP2') and third ('RP3') sequential radical pairs are extremely similar and mainly reflect the singlet state bleaching of the primary donor P_{700} [130]. If the accessory chlorophylls were involved in the radical pair formation, they should be expected to contribute to the SAS as an additional chlorophyll bleaching. The only SAS in which a bleaching of more then one chlorophyll ground state is observed is the one associated with the first 'RP1'. A possible explanation of the observation is to consider that the charge separation can actually take place from one of the accessory chlorophylls [130]. Given the similarity of the SAS presented in [130], this proposition would hold only given that the absorption spectra of the chlorophyll from which the charge separation is initiated and the one which carries the excited state character in the secondary radical pair ('RP2') are essentially identical. At the present level of understanding of the system, this hypothesis cannot be ruled out; on the other hand, a more straightforward interpretation, which has been discussed but not analysed in Ref. [130], is that the additional radical pair observed for the first time in their study might reflect the formation of identical states on each of the electron transfer branches of the PS I reaction centre. In fact, Ramesh et al. [140] have reported the accumulation of an optical transient signal attributed to A_0 in the hundred of picosecond timescale, as a result of ligand substitution to the primary chlorophyll acceptor, either on the PsaA or the PsaB reaction centre subunit. We have therefore, in the absence of unambiguous proof of the involvement of the accessory chlorophylls as electron transfer intermediates, attempted to model the observed decay lifetime reported by Muller et al. [130], which is, to our knowledge, the most refined model-based analysis present in the literature in terms of the bi-directional electron transfer hypothesis. These authors have also considered a reversible charge separation [130], in order

to describe the fluorescence decay [118,119,123,131–136], and this has also been included in the kinetic model used here for electron transfer simulations.

Fig. 1 shows the simple and more elaborate mono-directional kinetic models for charge separation and primary radical pair formation in PS I, as revised by Muller and coworkers, and the bi-directional one considered in the present study. The kinetic rate constants, in units of ns^{-1}, together with the resulting lifetimes (the eigenvalues of the system of differential equations) are also presented in the diagram. The evolution of the antenna excited state, the primary radical and the rise of the secondary radical pairs formed on both the PsaA and the PsaB branches of Photosystem I reaction centre are presented in Fig. 2.

The model simulations presented in Fig. 2 were obtained setting the same value for primary charge separation on both the electron transfer branches. This is based on the observation that the edge-to-edge distances between the Chl *a*, identified as the primary acceptor A_0 on the PsaA and the PsaB reaction centre subunits, and the Chl *a* and Chl *a*′ that constitute the so-called P_{700} dimer are almost identical. The value for the rate constant which appears to describe the experimental result 100 ns^{-1} is, at a first glance, similar to the about $(10–20\ ps)^{-1}$ suggested by several laboratories [17,113,114,124,126,128,137–139], but significantly smaller than the value, about 400 ns^{-1}, proposed by the Holzwarth group [130]. However, taking into consideration that a bi-directional electron transfer model is considered here, an overall charge separation rate of about 200 ns^{-1} is actually obtained, which appears to be an intermediate value between the ~100 ns^{-1} and the ~400 ns^{-1} values. Detailed model calculations of exciton equilibration in the Photosystem I antenna have been pursued in several studies, and it has been shown that the rate of exciton trapping is strongly dependent on the stoichiometry and the energy difference between the bulk antenna, which are almost isoenergetic with P^*_{700}, and the 'red absorption–emission' forms of Photosystem I (e.g., [102,107,110,118,130]). Therefore, we consider the value for the rate of primary charge separation presented in this study as a reasonable approximation only, given that a detailed attempt to model the excited state

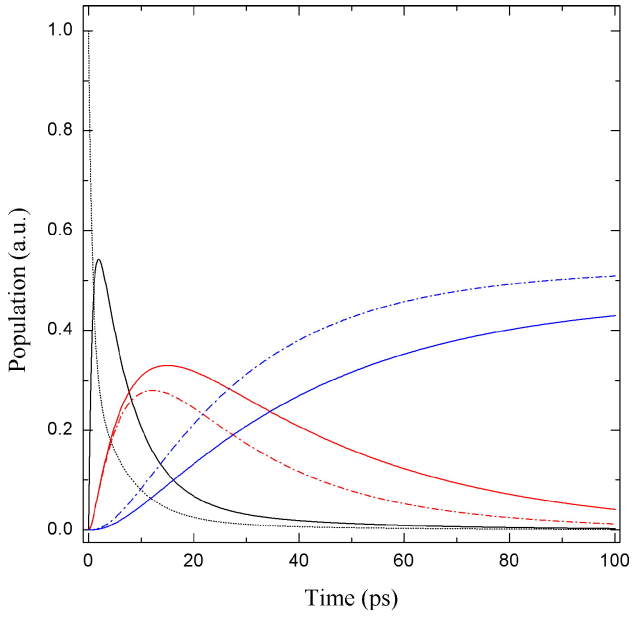

Fig. 2. Population evolution of the bulk antenna (black, dotted line), the excited state of the primary (black, solid line) donor, and the primary radical pairs $[P^+_{700}A^-_{0A}]$ (red, solid line) and $[P^+_{700}A^-_{0B}]$ (red, dash-dotted line). The initial rises of the secondary radicals pairs $[P^+_{700}A^-_{1A}]$ (blue, solid line) and $[P^+_{700}A^-_{1B}]$ (blue, dash-dotted line) are also shown. The kinetic constants and the characteristic lifetimes are the same as those indicated in the legend of Fig. 1 for model C.

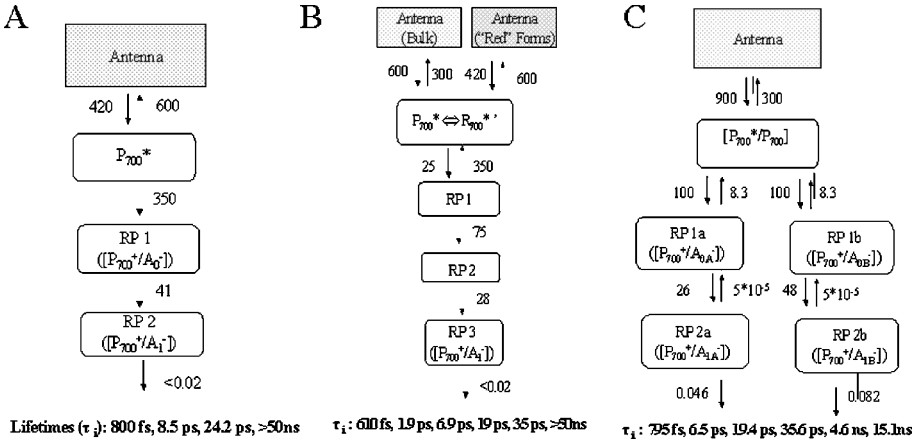

Fig. 1. Kinetic model of primary reactions in Photosystem I. (A) Transfer-to-trap limited model, as modified by Muller et al. [130], considering two consecutive radical pair states (RP1 and RP2). For the sake of consistency, these 'RP1' and 'RP2' have been assigned to $[P^+_{700}A^-_0]$ and $[P^+_{700}A^-_1]$. (B) The refined electron transfer model proposed by Muller and coworkers, including energy transfer from different antenna population and three (not unambiguously identified) radical pair states which include the reversible primary charge separation. (C) The bi-directional electron transfer model employed in the calculations presented in the manuscript. Primary radical formation is considered reversible. Also reported in the figures are the kinetic rates in units if ns^{-1} and the resulting decay lifetimes (eigenvalues) of the system, for all the three kinetic models. The values for model A and B are taken from [130].

equilibration phenomena between P^{*}_{700} and the antenna has not been pursued in the present study.

The numerical simulation results in close weighted average rise times of 8.9 ps and 6.5 ps for the $[P^{+}_{700}A^{-}_{0A}]$ and the $[P^{+}_{700}A^{-}_{0B}]$ radical pairs, respectively, which fall in the rather broad 6–9 ps lifetime distribution observed in the ultrafast optical absorption measurements [130]. Slightly different values for the rise time of the $[P^{+}_{700}A^{-}_{0}]$ and the $[P^{+}_{700}A^{-}_{1}]$ radical pairs on the PsaA and PsaB branches are calculated, as a result of different weighting factors (eigenvectors) in the presence of the same lifetimes (eigenvalues). The rise of $[P^{+}_{700}A^{-}_{0B}]$ is monotonous and is associated with the 6.5 ps lifetime, while the rise of the $[P^{+}_{700}A^{-}_{0A}]$ radical pair is biphasic with lifetimes of 6.5 ps and 19 ps, the former accounting for 0.8 of the normalised amplitude. The observation of a non-monotonous rise phase is an expected result, as all the stages in the electron transfer chain would contribute a component. The decay of the $[P^{+}_{700}A^{-}_{0A}]$ and the $[P^{+}_{700}A^{-}_{0B}]$ radical pairs is described by three main lifetimes of 795 fs, 19 ps, and 35 ps. The 35 ps lifetime component dominates the decay of the $[P^{+}_{700}A^{-}_{0A}]$ radical pair, being associated with a normalised amplitude of 0.9. The resulting weighted averaged decay lifetime for this radical pair is 32.6 ps. The $[P^{+}_{700}A^{-}_{0B}]$ decay is described mainly by the 19 ps and the 35 ps lifetimes, which have normalised amplitudes of 0.7 and 0.2 respectively, yielding a weighted average lifetime of 21 ps. The results of our simulations seem in general agreement with most of the data reported in the literature obtained by ultrafast absorption measurements, which indicate a decay in the 20–40 ps interval (reviewed in [102,124]), a value that also reflects the main fluorescence decay component in PS I preparations from this organism of 36 ps [125]. It is apparent that the two primary radical pairs evolve with similar temporal and spectral dynamics, and this could be the reason why a distinct contribution from $[P^{+}_{700}A^{-}_{0A}]$ and $[P^{+}_{700}A^{-}_{0B}]$ was not observed directly [130]. Moreover, all these values for the electron transfer constants are estimated so that the decay lifetimes fall within a lifetime distribution, rather than to a single defined value, hence closely lying components might be masked by the overlap of lifetime distributions. It should also be noted that the transient spectra reported by Ramesh et al. [140] for the chlorophylls attributed to A_{0A} and A_{0B} do not show major differences, at most a slight shift in the peak position, suggesting that the species associated spectra (SAS) for the $[P^{+}_{700}A^{-}_{0A}]$ and the $[P^{+}_{700}A_{0B}]$ radical pair would not be distinguishable.

Also presented in Fig. 2 are the initial rise kinetics for the secondary radical pairs $[P^{+}_{700}A^{-}_{1A}]$ and $[P^{+}_{700}A_{1B}]$, which exhibit weighted average lifetimes of 35.5 ps and 25.0 ps, respectively. The values reflect the two lifetime distributions of ~20 and ~40 ps described by Muller at al. [130] and which have been associated with the evolution of 'RP2' and 'RP3' in their kinetic model (see Fig. 1B). These are the radical pairs which show a very similar SAS strongly dominated by the bleaching of the primary donor P_{700}. This observation supports the suggestion presented here that these species associated spectra could represent the $[P^{+}_{700}A^{-}_{1A}]$ and $[P^{+}_{700}A_{1B}]$ radical pair, as no significant contribution of the phylloquinone A_1 is expected in the difference spectrum in the 600–800 nm wavelength region, and the P^{+}_{700} would be the same for both radical pairs. The $[P^{+}_{700}A^{-}_{1}]$ radical pair can be distinguished from the $[P^{+}_{700}A^{-}_{0}]$ radical pair because of the relative larger spread in the centre of the lifetime distribution. The rise time for the $[P^{+}_{700}A^{-}_{1A}]$ and $[P^{+}_{700}A_{1B}]$ species are also in full agreement with ultrafast studies of quinone reduction, which have estimated a rise time of about 38 ps [23]. In photovoltage studies, which also provide estimates of the rise time of the radical pair couple providing that the event is electrogenic, two phases of about 20 to 50 ps have been detected and assigned to the sequential reduction of $A_{0(A)}$ and $A_{1(A)}$ [15,141]. In view of the model and calculations presented in this study and the direct evidence for the primary radical pair rising in about 6–9 ps, the photovoltage results can be interpreted in view of heterogeneous phases of A_1 reduction with rise lifetimes of ~20 and ~35 ps.

3.1.1. Further considerations on the relationship between the rate of primary charge separation and electron transfer tunnelling theory

In the previous section, we have discussed some models for primary charge separation events and discussed them merely on the basis of the electron transfer reactions. In this section, their relationship to the electron transfer tunnelling theory and the thermodynamic properties of the system will be discussed.

Values in the range of $(1 \text{ to } 10 \text{ ps})^{-1}$ were reported for the rate of primary photochemistry (k_{fc}) in PS I [17–19,47,120,124–126,128–130,137–139], and suggestions for even faster rates in the order of several hundred of femtoseconds have been also advanced [47,102,107,112,142,143]. In the numerical simulations described in the previous section, which to our knowledge, for the first time, explicitly considered a bi-directional model for charge separation and which are widely based on the results of Ref. [130], a rate for primary charge separation of about $(10 \text{ ps})^{-1}$ on each electron transfer branch is obtained. The primary donor P_{700} is generally thought of as a Chl *a* Chl *a*′ heterodimer, even though electronic coupling with other chlorophylls need to be considered in order to described the complexity of the $[P_{700}-P^{+}_{700}]$ [113,114,116,156] and $[P_{700}-P^{3}_{700}]$ [144–148,156] difference spectra [149]. The accessory chlorophylls are located at a centre to centre distance of about 12 Å from each partner of the so-called primary donor heterodimer [3]. This, in turn, can be taken as an indication that the excited state character can be diffused over more than the 'dimer-proper' and P_{700} could be represented as a weakly coupled four-degenerated Chl multimer. Due to the relatively short edge-to-edge distance between P_{700} and the accessory Chls (~4.7 Å), it has been suggested that they might take part in the electron transfer

events, although even with extremely high temporal resolution, an electron transfer event associated with this Chl has not been unambiguously demonstrated. However, an electron transfer event, which would by-pass the accessory Chl in favour of direct transfer to the $A_{0,}$ requires some further discussion. As previously mentioned, no attempt to accurately describe the excited state equilibration and rate of transfer to the trap has been made in our simulation, therefore, the $(10\ ps)^{-1}$ charge separation rate should be viewed as only as an approximation. Moreover, in our simulation, only population from the bulk antenna which lay at higher energy compared to the reaction centre proper [103] has been taken into consideration. Therefore, the value obtained should be considered on the verge of the higher limit (lower value) for charge separation. The edge-to-edge distance between the A_0, which is considered as the primary acceptor, and one half of the dimer-proper is 9.7 Å on the PsaA subunit and 9.8 Å on the PsaB subunit [3]. Even under optimal electron transfer conditions when $\Delta G = -\lambda$ [83,85,86,90], the electron transfer rate obtained over such a distance between electron donor and acceptor is in the range of $1\ ns^{-1}$, hence about two orders of magnitude slower than the one derived by the numerical simulation. Moreover, a condition of $\Delta G = -\lambda$ is not expected in this situation since, from the equilibrium rate constant of reversible charge separation, which is that described by Holzwath and coworkers [130], a free energy difference of −65 meV is estimated. This is a smaller value than the −180 to −250 meV estimated from the kinetics of delayed luminescence [94–96,150], and we will discuss this aspect further later. Therefore, it can be concluded that either the Moser–Dutton [85,90] approximation cannot be considered as valid in the case of PS I electron transfer events or that the assumption of electron transfer directly from P_{700} to A_0 does not provide a correct description of primary electron events. Two possible scenarios can reconcile the values for electron transfer rates reported in the literature and that obtained by the numerical simulations presented in this manuscript, in the frame of electron tunnelling theory:

1) P_{700} is effectively a Chl *a* multimer, which includes the accessory chlorophylls, and A_0 is a monomeric Chl. In that case the edge-to-edge distance between P^*_{700} and A_0 can be approximated by the one between the accessory Chls and A_0 (~3.7 Å). In this assumption, the maximal rate calculated for electron transfer is $7.5\ ps^{-1}$, which is within the range of the faster estimates for the rate of primary photochemistry reported in the literature [47, 102,107,112,142,143].
2) A_0 as well as P_{700} are Chl dimers. In Fig. 3 are presented the cofactor arrangement based on the *S. elongatus* structure [3] for one electron transfer branch, in a view perpendicular to the normal plane and rotated around the symmetry axis, to show the possible arrangement of A_0. For this configuration, within the point dipole approximation [151, 152] and assuming site energy equivalent to the wavelength of 700 nm for the primary donor and 690 nm for the accessory Chl and the Chl assigned as A_0, we calculate an excitonic interaction energy of $320\ cm^{-1}$ for the radical pair dimer, ~$255\ cm^{-1}$ for A_0/A_{cc}, and ~$80\ cm^{-1}$ for A_{cc}/P_{700}. However, the assumption of point dipole might be not entirely representative for molecules which have edge-to-edge distances close to the van der Waals radius [153]. Refined calculation which considers both the extended dipole approximation and different site energies for each of the chlorophylls molecule surrounding the reaction centre (i.e., P_{700}, A_{acc}, and A_0, as derived from the description of the $[^3P_{700}-P_{700}]$ and $[P^+_{700}-P_{700}]$ difference spectra) results in estimates of the excitonic coupling within the reaction centre "proper" of $157\ cm^{-1}$ and of ~$136\ cm^{-1}$ between A_0 and the accessory Chl [149]. Therefore, it appears that both approaches yield an excitonic coupling between A_0 and the accessory Chl, which is larger than that estimated for the accessory and the accessory and the primary donor dimer proper.

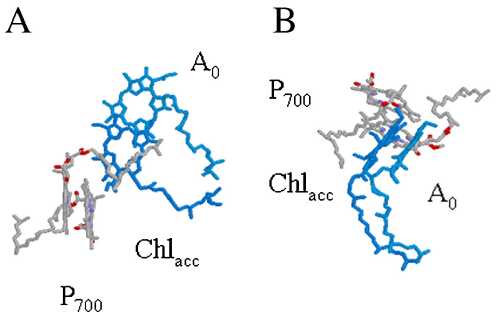

Fig. 3. Arrangement of the Chls attributed to the P_{700} 'special pair' (grey carbon backbones), and the Chl_{ACC} and A_0 (cyan carbon backbone) on the PsaA subunit of the reaction centre, in a view perpendicular to the membrane plane (A) and rotated along the A_0-Chl_{ACC} (B) in order to emphasise the possible dimeric organisation of the latter cofactors.

It should be noted that while recently A_0 has been widely accepted to be monomeric in nature [10,16,70,121,154, 155], early reports by Shuvalov and coworkers [9,13] had suggested a possible dimeric organisation of this electron transfer intermediate. If that were the case, the edge-to-edge distance between P^*_{700} and A_0 can be considered as ~4.7 Å. Also, in this case, the maximum possible rate constant, obtained from the Moser–Dutton approximation, is of $2.5\ ps^{-1}$, which is in the range of commonly accepted values for charge separation, although it is calculated for ideal energetic conditions. If the free energy of −65 meV is taken into account, a rate of $100\ ns^{-1}$ is obtained when λ assumes a value of 0.5 eV, which again is a realistic value.

It can be seen that both these hypotheses can provide a reasonable description of the primary electron transfer rates modelled and the values reported in the literature. We tend to prefer the second hypothesis due to larger excitonic coupling estimates between the accessory Chl and (so-called) Chl A_0 rather than P_{700} and the accessory, although

the value calculated can be considered only as a first approximation, therefore Hypothesis 1 cannot be completely excluded and further experimental evidence will be needed to fully characterise primary charge separation events in PS I.

3.2. Electron transfer events in the nano- to microsecond time scale: secondary radical pairs and electron transfer to the iron–sulfur cluster F_X

The rate of reduction of the iron–sulfur cluster F_X by the phylloquinone A_1 has often been reported to be biphasic, with apparent lifetimes ranging in the tens to hundred of nanoseconds [36–38,47,59]. Recently, it has been possible to monitor two phases of phylloquinone reoxidation, associated with decay lifetimes of about 20 ns and 250 ns. A modified kinetic model based on the one originally proposed by Joliot and Joliot [36], which condenses the more recent reports [38] and considers all the electron transfer reactions as essentially irreversible, is presented in Fig. 4. It should be remembered that the assumption that electron transfer reactions are essentially irreversible applies only in the case in which the rate constant for the forward reaction has a much larger value than the one for the backward reaction, a factor which is determined by the thermodynamic properties of the system. As this can't be assumed a priori, we also employ a kinetic model which explicitly takes into consideration the equilibrium between both phylloquinone molecules A_{1A} and A_{1B} and F_X, which is presented in Fig. 4C.

In the kinetic model presented in Fig. 4C, the parameters which need to be refined in order to describe the experimental observables are the driving forces for the reduction of the Fe–S centre F_X by the PsaA- and PsaB-bound phylloquinones. These determine the forward and backward rates of the reaction, as well as the rate of reoxidation of F_X by F_A, which, as a first approximation, represents the output rate of the system. For the sake of clarity, these two aspects are discussed separately, even if it is apparent that they need to be simultaneously adjusted in order to obtain a satisfactory description of the population evolution of the electron transfer intermediates.

3.2.1. Effect of altering the free energy of the A_{1A} and A_{1B} reoxidation reactions on the evolution of the $[P^+_{700}A^-_{1A}]$ and the $[P^+_{700}A^-_{1B}]$ radical pair populations

While the maximum rate of electron transfer is influenced by both the reorganisation energy and the Gibbs free energy [83,84,86], only the latter is linked to the equilibrium constant. Moreover the experimental estimation of λ is often, if not always, more uncertain than the one of ΔG^0 which can be addressed when feasible by the estimation of redox midpoint potential of the electron transfer cofactor by direct titration. Therefore, as a first approximation, we limit our discussion here to the effect of the redox potential of the PsaA and PsaB bound phylloquinones. However, the consequences of altering the value of the reorganisation energy will be considered at a later stage.

The redox potentials for the two phylloquinones located in each putative electron transfer branch were recently calculated, estimating the electrostatic energies from the solution of the Poisson–Boltzmann equation based on the crystal structure [82]. The estimated redox potential for the PsaA-bound phylloquinone is −531 mV, and the one for the PsaB-bound phylloquinone is −686 mV [82]. These values are in sharp contrast to previous indirect estimates based on the experimental approach of quinone substitution and application of Marcus theory for electron transfer, which had predicted a more negative potential at least for the A_{1A} quinone of about −820 mV [80]. Interestingly, a direct

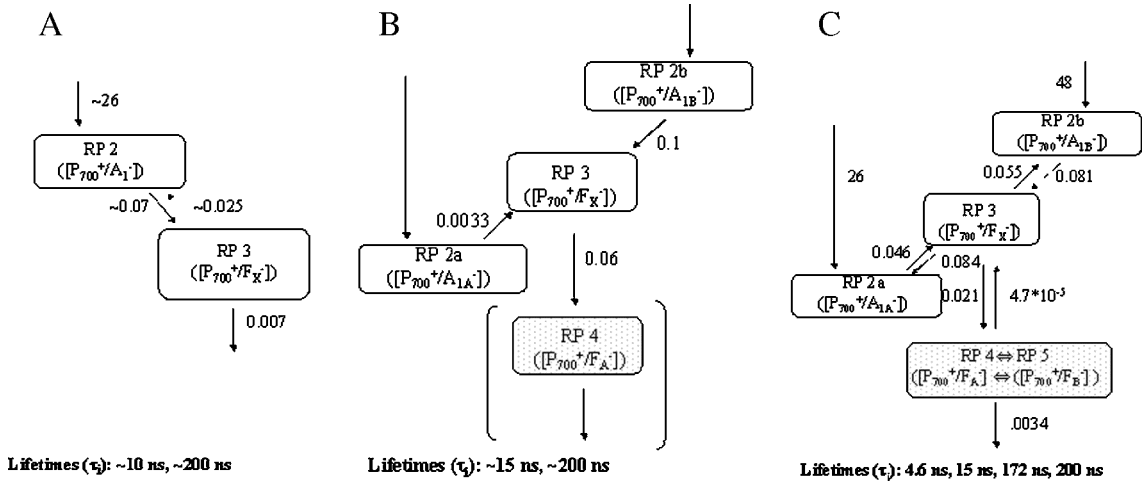

Fig. 4. Kinetic model of the electron transfer reactions involving phylloquinone A_1 reoxidation and the iron–suphur cluster F_X reduction in Photosystem I. (A) The mono-directional "shallow" equilibrium model originally proposed by Brettel and Setif [19,59,60]. (B) Bi-directional electron transfer model for A_1 reoxidation originally proposed by Joliot and Joliot [36] and as modified by Agalov and Brettel [38]. (C) Bi-directional electron transfer model which explicitly takes into account the equilibrium between A_{1A}, A_{1B}, and F_X. Also reported in the figure are the kinetic rates in units of ns^{-1} and the approximated and computed decay lifetimes of the system for all the three kinetic models.

estimation of the redox potential for one of the quinones of −540 mV has been reported by Munge et al. [93], by cyclic voltametry of PS I particles embedded in liposome films, which is not dissimilar from the potential for the PsaA phylloquinone estimated by the Poisson–Boltzmann equation. On the other hand the same authors reported an extremely positive redox potential for the terminal iron–sulfur centres $F_{A/B}$ of −190 mV [93], which is about 350 mV more positive than the value determined by EPR titration [24,25,42,43,74,158]. Since the estimation of midpoint potential can be somewhat distorted by interface phenomena at the electrode, it is not unreasonable to consider that only the estimated energy gap between A_1 and $F_{A/B}$ is reliable in these measurements, as is also acknowledged and discussed by the authors [93]. When the midpoint potential of A_1 is downshifted by the difference between the midpoint potential estimates by film voltammetry and either optical or EPR titration of the $F_{A/B}$ centres, a value in the −790 to −890 mV interval is obtained, which is in the range derived from quinone substitution [80], but disagrees with calculation based on the protein–cofactor electrostatic interactions [82]. Therefore, it is apparent that there are still broad uncertainties about the correct redox potential of A_1.

The value of the redox midpoint potential of the iron–sulfur cluster F_X was estimated in the −(660–730) mV range [75–78]. The reduction of F_X can be predicted to be significantly exergonic, if the −820 mV value estimated by Itoh and coworkers [80,81] for the phylloquinone redox couple is considered. However, if the values of midpoint potentials computed by the solution of the Boltzmann–Poisson equation were correct, then this electron transfer reaction would be endergonic and take place against a rather large difference in electrical potential energy of about 150 meV [82]. Brettel and coworkers [53] have shown that about a half of the PS I centres are incapable of forward electron transfer from $A_{1(A)}$ to F_X at temperatures below the protein matrix/glass transition. The activation energy for this electron transfer reaction has been estimated at about 110–220 meV [19,38,47,53]. This is in fairly good agreement with the prediction of a thermally activated electron transfer between A_1 and F_X. A refined analysis of the temperature dependence of A_1 reoxidation with a temporal resolution high enough to resolve the fast component has shown that the ~20 ns phase is almost temperature independent, with an estimated activation energy of only about 15 meV [38], which would favour a model in which the electron transfer between A_{1B} and F_X is downhill or only slightly uphill. Both these situations would agree well with the calculated potential for the A_{1B}/A_{1B}^- redox couple and the spread of potential reported for F_X in the literature [75–78].

Therefore, we have used the E_m values for the phylloquinone A_{1A} and A_{1B} of −531 mV and −686 mV derived from the Poisson–Boltzmann calculations as initial estimates [82]. The calculated forward and backward constants for the electron transfer reaction, considering two different values of redox potential for F_X (−705 mV [75] and −660 mV [76]), and several values for the reorganisation energy λ in the range of 0.3 to 0.75 eV have been computed and are reported in Table 1.

However, when model calculations that include reversible equilibria are performed using the redox potential suggested in Ref. [82] for the PsaA phylloquinone, the $[P_{700}^+ A_{1A}^-]$ radical pair does not decay, even within a 10 μs window, and charge recombination reactions to either the singlet or the triplet state are ignored (not shown). It is therefore apparent that the redox potential of A_{1A} must be poised to a more negative value in order to satisfactorily simulate the experimental results.

A simulation which reasonably describes the experimental measurements of electron transfer reaction associated with the $[P_{700}^+A_{1A}^-]$, $[P_{700}^+A_{1B}^-]$, and $[P_{700}^+F_X^-]$ radical pairs is presented in Fig. 5. The population evolution of these radical pairs has been computed assuming a difference in redox potential of −15 mV between A_{1A} and F_X, +10 mV between A_{1B} and F_X, and considering the reorganisation energy as 0.65 eV. The resulting rate constants are also

Table 1
Rates of forward and backward electron transfer from A_{1A} and A_{1B} to F_X

	$(k_f)^{-1}ns^{-1}$	$(k_b)^{-1}ns^{-1}$	ΔG^1 eV (KT)	$(k_f)^{-1}ns^{-1}$	$(k_b)^{-1}ns^{-1}$	ΔG^2 eV (KT)
Reorganisation energy λ= 0.3 eV						
$A_{1A}\rightarrow F_X$	315.6	0.22	0.174 (7.26)	66.2	0.30	0.129 (5.38)
$A_{1B}\rightarrow F_X$	2.18	0.99	0.019 (0.79)	0.90	2.7	−0.026 (1.08)
Reorganisation energy λ= 0.5 eV						
$A_{1A}\rightarrow F_X$	985.9	0.68	0.174 (7.26)	235.7	1.1	0.129 (5.38)
$A_{1B}\rightarrow F_X$	9.1	4.11	0.019 (0.79)	3.74	11.0	−0.026 (1.08)
Reorganisation energy λ= 0.75 eV						
$A_{1A}\rightarrow F_X$	5083.5	3.55	0.174 (7.26)	1296.7	5.9	0.129 (5.38)
$A_{1B}\rightarrow F_X$	54.1	24.5	0.019 (0.79)	22.2	65.76	−0.026 (1.08)

The rates of forward and backwards electron transfer between A_{1A} and A_{1B} and F_X computed on the basis of the midpoint potential estimated by the solution of the Poisson–Boltzmann equation for the quinone potential (A_{1A}=−531 mV, A_{1B}=−686 mV) and considering two different published redox potential for F_X (−705 mV, defines ΔG^1 and −660 mV defines ΔG^2) are shown. The forward and backward rates of electron transfer has been weighted according to the Boltzmann distribution.

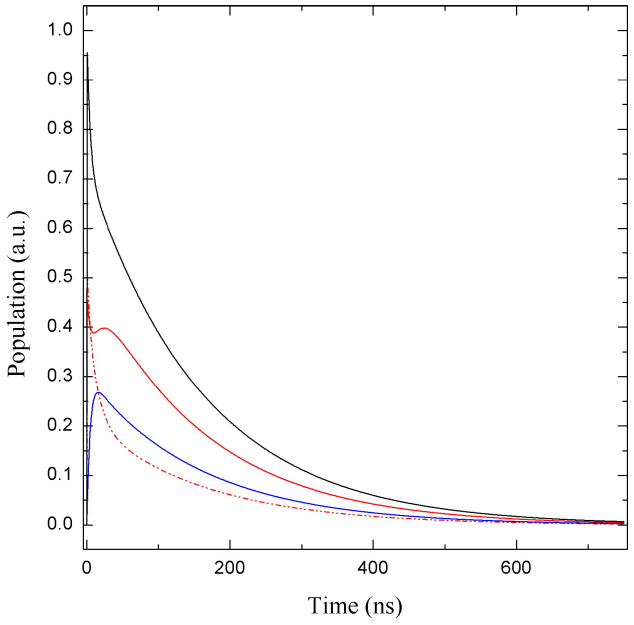

Fig. 5. Population evolution of the secondary radical pairs $[P^{+}_{700}A^{-}_{1A}]$ (red, solid line), $[P^{+}_{700}A^{-}_{1B}]$ (red, dash-dotted line), and $[P^{+}_{700}F^{-}_{X}]$ (blue, dotted line), calculated for ΔG^{0} values of 12 meV, −10 meV, and −155 meV, respectively, and considering an activation energy λ of 0.6 eV for both phylloquinone reoxidation reactions. The sum of the decay of $[P^{+}_{700}A^{-}_{1A}]$ and $[P^{+}_{700}A^{-}_{1B}]$, which is meant to represent the experimentally detectable kinetics, is also presented (black, solid line). The rate constants used in the simulation are reported in the kinetic scheme C of Fig. 5.

reported in the schematic kinetic model C of Fig. 4. The population evolution of the secondary radical pair $[P^{+}_{700}A^{-}_{1}]$ has been calculated as the sum of the population evolution of $[P^{+}_{700}A^{-}_{1A}]$ and $[P^{+}_{700}A^{-}_{1B}]$ and which therefore represents the actual experimental observable, also presented in Fig. 5. It should be stressed that due to the uncertainty in the estimates of both the reorganisation energy and the redox potentials of the cofactors, which are not fully independent variables, the value of ΔG^{0} presented here should be considered as a reasonable approximation and not as a precise estimate of the free energy gap between the redox cofactors. In fact, the reoxidation of $[P^{+}_{700}A^{-}_{1A}]$ and $[P^{+}_{700}A^{-}_{1B}]$ can be simulated well, assuming different combinations of values for the driving force and the reorganisation energy, which has been assumed to have the same values for both A_1 phylloquinone reoxidation reactions in the absence of any evidence to the contrary. Assuming reasonable values for the reorganisation energy (between 0.4 and 1 eV), the uncertainty about the driving force estimate is about 5–25 meV for both electron transfer reactions. It should be noted that, whatever precise value of the redox potential for phylloquinone is assumed, the redox potential difference between the phylloquinone molecules is in the range of 10 to 50 mV, which, at a first approximation, indicates that they are almost isoenergetic to F_X (Figs. 4 and 5).

The decay of the secondary radical pair $[P^{+}_{700}A^{-}_{1}]$ is described by four lifetime components of significant amplitude, the first of which is 6.5 ps and accounts for a normalised initial amplitude of about 0.25 and would not usually be resolved in the experimental measurements. The other decay lifetimes fall in the nanosecond time range and have values of 4.7 ns, 172 ns, and 199 ns. Their associated normalised amplitudes are 0.22, 0.38, and 0.16, respectively. This, in turn, yields a weighted average decay lifetime of 100 ns for the $[P^{-}_{700}A^{-}_{1}]$ radical pair. If the pisecosecond component which is not experimentally resolved but emerges in the simulation, due to the kinetic coupling with the upstream electron transfer reaction, is excluded from the τ_{av} calculation, a value of 130 ns is obtained. This is not dissimilar from the value of 100–150 ns that is computable considering two equally weighted lifetimes components of about 5–20 ns and 150–300 ns obtained by optical transients associated with A_1 reoxidation [19,36,47,59,60]. It is also interesting to notice that Agalov and Brettel have reported that the reoxidation of A_1 in the nanosecond time range [38] is better fitted by a combination of three exponential functions showing about the same value for lifetimes and pre-exponential weight modelled in our calculations. However, these authors were unable to further characterise the third kinetic component. Also presented in Fig. 5 is the decay of the $[P^{+}_{700}F^{-}_{X}]$ radical pair, which rises with an average lifetime of 4.7 ns, which essentially matches the fast decay lifetime of the $[P^{+}_{700}A^{-}_{1}]$ reoxidation. This is in the range of the instrument limited response of photovoltage set-ups (e.g., [15,141,159]), therefore agreeing with resorts that this electrogenic reaction is not kinetically resolved in these types of measurement. The decay of $[P^{+}_{700}F^{-}_{X}]$ is described by three main lifetime components of 15, 172 ns and 199 ns, associated with normalised amplitudes of 0.16, 0.58 and 0.25. This, in turn, yields an average lifetime of 155 ns. From the model calculations, it can be noted that $[P^{+}_{700}F^{-}_{X}]$ and $[P^{+}_{700}A^{-}_{1}]$ radical pairs decay in very close time intervals; however, the effective population concentration of $[P^{+}_{700}F^{-}_{X}]$ disappears earlier due to the relatively low initial amplitude for this radical pair state (Fig. 5).

It is worthwhile to emphasise that, in general, but more clearly, in the case of the $[P^{+}_{700}A^{-}_{1A}]$ radical pair, the estimated average lifetime differs from the estimated rate constant. In the latter case, while the F_X reduction rate by A_{1A} is estimated by tunnelling at $(21.6\ \text{ns})^{-1}$, the average decay lifetime for the radical pair has a value of about 115 ns and lifetime components in the nanosecond range (172 ns and 199 ns) are also obtained. This is the result of the population equilibrium between the two radical pair states involving the phylloquinones and the iron–sulfur cluster F_X, but is a more general feature of coupled electron transfer reactions for which the experimentally observable lifetimes might not necessarily reflect the intrinsic reaction rate constant.

Some of the more stringent evidence which has led to the suggestion of bi-directional electron transfer in PS I was obtained by site directed mutagenesis of conserved residues in the quinone binding site. Many of the mutations have

been directed toward the tryptophans that provide the π–π stacking to the napthoquinone ring [37]. A relatively conservative mutation to a phenylalanine had the effect of lengthening the lifetime of $[P_{700}^{+}A_1^{-}]$, so that mutation on the PsaB subunit shifted the lifetime of the fast phase from ~19 ns to ~95 ns, while the mutation on the PsaA subunit shifted the lifetime of the fast phase from ~205 ns to ~580 ns [37]. Less conservative mutations for the tryptophan on the PsaA reaction centre subunit, to either a histidine or a leucine, result in an estimated decay of the $[P_{700}^{+}A_{1A}^{-}]$ radical pair of about 1.2 μs, which is about one order of magnitude slower than the value measured in the wild-type [58]. The results obtained by site directed mutagenesis can be explained by the kinetic model, considering the equilibrium between both phylloquinones and F_X and only assuming a change in the energetics of the reaction, and simulations of some of the effects of the mutations previously discussed are presented in Fig. 6. It should be noted that the changes in the redox potentials are not the only factors determining the electron transfer rates, and that changes in the reorganisation energy, protein packing density, and especially distances would have a significant effect as well. Although this should be considered as a first approximation, we have performed an extended investigation of the effect of modulating the driving force for the reduction of F_X by either the bound phylloquinone A_{1A} or A_{1B} on the value of the decay lifetime usually associated with A_1 reoxidation. The mean distribution lifetime ($\bar{\tau}$) for

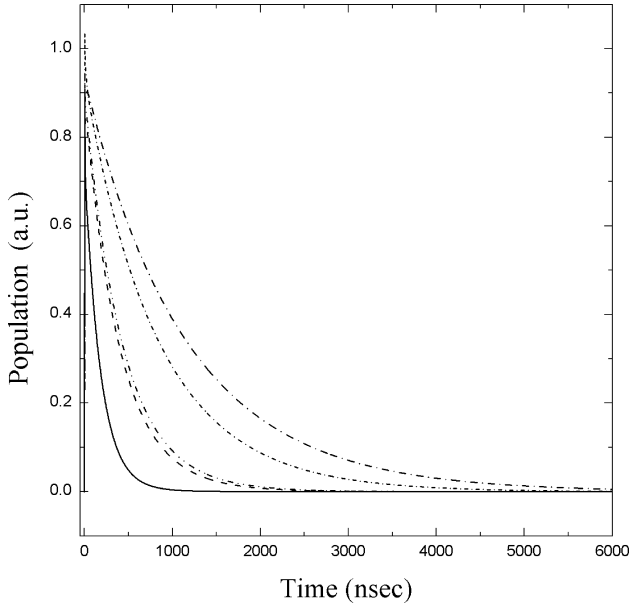

Fig. 6. Model simulations of the decay of the $[P_{700}^{+}A_1^{-}]$ radical pair that describe some of the point mutations in the A_1 quinone binding site, obtained by changing the redox potential of the phylloquinones. Solid line: wild-type, $\Delta G^0_{A1A/FX}$=12 meV, $\Delta G^0_{A1B/FX}$=−10 meV; dotted line: PsaA-W663F [37], $\Delta G^0_{A1A/FX}$=55 meV; dashed Line: PsaA-W663H [58], $\Delta G^0_{A1A/FX}$=85 meV; dotted line: PsaB-W673F [37], $\Delta G^0_{A1B/FX}$=50 meV; dashed Line: PsaB-W673H [51], $\Delta G^0_{A1B/FX}$=75 meV.

both quinones is presented in Fig. 7, when a fixed value for the λ is considered. The driving force for the reaction has been varied on both electron transfer branches in a range of ±0.1 eV. The interval of difference in redox potential values between A_{1A} and F_X and A_{1B} and F_X, which can be considered as acceptable within the uncertainty in the estimate of electron tunnelling parameters and the spread of lifetimes reported in the literature, are also highlighted in Fig. 7.

Altering the redox potential of only one of the two phylloquinones affects the dynamics of electron transfer reactions involving both due to the relatively small driving force associated with this electron transfer step on both electron transfer branches of the reaction centre. When the potential of the A_{1B}/A_{1B} redox couple is modulated, assuming a fixed value for the Fe–S cluster F_X within the exergonic to isoenergetic range, only a relatively moderate effect on the kinetics of A_{1A} quinone reoxidation is observed. However, a more pronounced "indirect effect" on the reoxidation rate of A_{1A} is modelled when the driving force associated with F_X reduction from A_{1B} is shifted to the endergonic range. The same consideration holds for the manipulation of the redox potential of A_{1A} on the kinetics of the $[P_{700}^{+}A_{1B}^{-}]$ radical pair couple (Fig. 7).

3.2.2. *Effect of altering the rate of F_X reduction on the $[P_{700}^{+}A_{1A}^{-}]$ and the $[P_{700}^{+}A_{1B}^{-}]$ radical pairs population evolution*

As previously discussed, the other important variable in the kinetic model presented here is the rate of oxidation of the iron–sulfur centre F_X. The direct measurement of the rates of reduction and oxidation of the iron–sulfur clusters $F_X/F_A/F_B$ is often impaired because of the very similar absorption spectra of the clusters, the relatively low extinction coefficient of the clusters, and the fact that the absorption spectrum is overlapped with the bulk absorption of chlorophylls and carotenoids that act as antenna pigments. Nonetheless, the rate of electron transfer and the electron transfer have been investigated in a series of experiments in which either the terminal Fe–S clusters F_B or both the F_A and F_B clusters are removed by chemical treatment [31,39,41,160–168]. This series of experiments have been the subject of extensive reviews by Brettel [19] and Leibl and Brettel [47].

Based on the $A_{1(A)}$ F_X equilibrium model [19,47,59], rates of $(\sim 80\ \text{ns})^{-1}$ for the higher plant PS I preparation and $(\sim 170\ \text{ns})^{-1}$ in a cyanobacterial PS I preparation have been suggested for F_X reduction by $A_{1(A)}$ [19,47,163]. However, it was not possible to directly observe a kinetic phase associated with the electron transfer from A_1 to F_X in photovoltage measurements [141]. This has been interpreted as an indication that F_X reoxidation by F_A is significantly faster than the reduction of F_X by A_1, and the rate constant for the former reaction has been estimated to be faster than $(50\ \text{ns})^{-1}$ [141]. A somewhat larger value for the forward

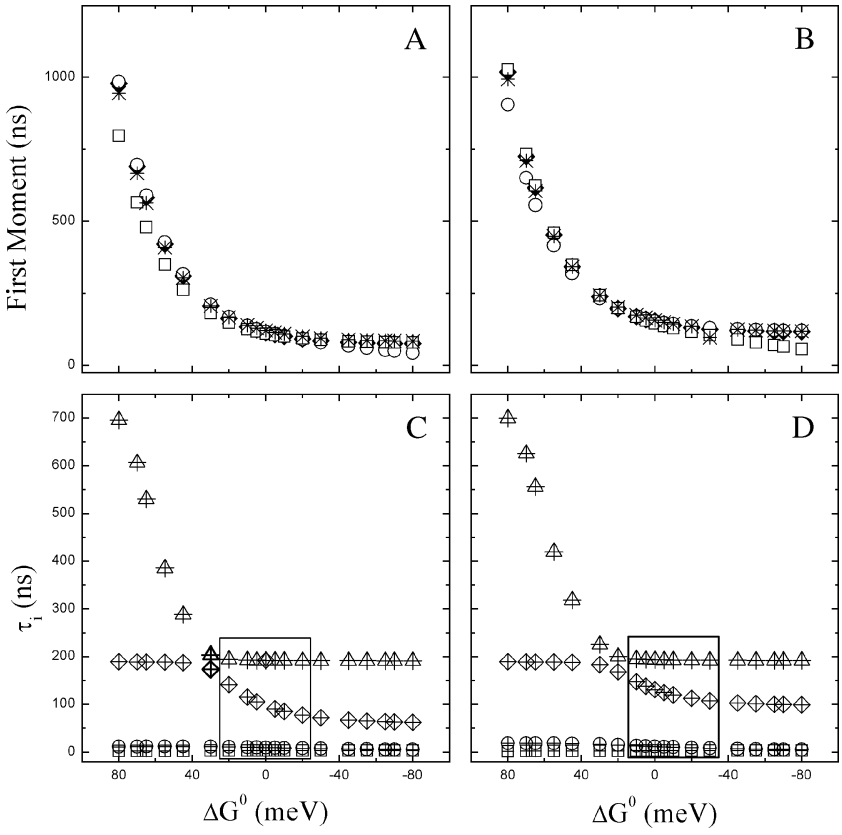

Fig. 7. The effect of systematically altering the redox potential of the A_{1A} (A) and the A_{1A} (B) phylloquinones on the observed mean decay lifetimes of the $[P^+_{700}A^-_{1A}]$ (open circles), the $[P^+_{700}A^-_{1A}]$ (open squares), the $[P^+_{700}F^-_X]$ (stars), and the $[P^+_{700}A^-_1]$ (full diamonds) radical pairs. The effect of systematically altering the value of redox potential of the A_{1A} (C) and A_{1B} (D) phylloquinone on the modelled decay lifetimes τ_i is shown. Crossed-centred squares: "~5 ns" lifetimes; crossed-centred circles: "~10 ns" lifetime; crossed-centred diamonds: "~160 ns" lifetime; crossed-centred triangles: "~200 ns" lifetime. The hyphenated values indicate the approximated experimentally estimated lifetimes. The boxes highlight the range of acceptable redox potentials for the A_{1A} and A_{1B} phylloquinones.

electron transfer from F_X to F_A of about $(25\ ns)^{-1}$ has been suggested by Joliot and Joliot [36].

Taking the edge-to-edge distances between the centres assigned to F_X and F_A in the crystal structure of 11.6 Å, and assuming that the driving force equals the reorganisation energy so that the electron transfer is optimised, a rate of $(6.3\ ns)^{-1}$ can be computed. That is about one order of magnitude faster than any of the previously suggested rates. Due to the spread in the published redox potentials for both the iron–sulfur centres F_X and F_A, obtained by monitoring the titration either by optical or electron paramagnetic resonance spectroscopy, a rather wide range of values for the driving force of the process lying between 120 and 265 meV need to considered in the calculations [31,39,41,160–168]. It should be noted that redox potential estimates obtained by the same techniques, i.e., EPR at low temperature [74,75,169] or optical titration at room temperature [76,79], are consistent in yielding a potential gap of about 120–150 mV between F_X and F_A. Moreover, a difference in the redox potential larger that 165 mV is inconsistent with the temperature dependence of charge recombination of $[P^+_{700}F^-_X]$ under conditions when F_A/F_B is pre-reduced or removed, and which is thought to proceed via the thermal reactivation of $A_{1(A)}$ [47,157]. The value of the forward electron transfer rates between F_X and F_A calculated for three representative values of ΔG and values of the reorganisation energy which fall in the range of the value reported in the literature for electron transfer proteins are reported in Table 2. It can be seen that, excluding the case of rather large but not spectacular values for the reorganisation energy, the estimated forward rates are in the range of values previously reported based on the kinetic experiment analysis. Remarkably, due to the large value of ΔG, this electron transfer step can be considered virtually irreversible. In the simulation presented here, an intermediate value for the rate constant of $(47.8\ ns)^{-1}$ has been obtained considering a Gibbs free energy of −155 meV, which is in the middle range of values reported in the literature, and λ has been set to an intermediate value of 0.55 eV.

The effect of altering the rate of F_X oxidation by modulating the value of λ, so that the equilibrium constant for the reaction is not altered, is illustrated in Fig. 8, where the dynamics of the $[P^+_{700}A_{1A}]$ and $[P^+_{700}A_{1B}]$ populations are presented as calculated for F_X reoxidation rates in the $(10\ ns)^{-1}$ to $(100\ ns)^{-1}$ range. The mean decay lifetimes of both the $[P^+_{700}A^-_1]$ and the $[P^+_{700}F^-_X]$ radical pairs are strongly

Table 2
Rates of forward and backward electron transfer from F_X to F_A

$F_X \rightarrow F_A$	$(k_f\ ns)^{-1}$	$(k_b\ \mu s)^{-1}$	ΔG eV (KT)
Reorganisation energy λ = 0.4 eV			
	25.5	2.66	−0.120 (4.65)
	16.9	10.1	−0.165 (6.39)
	8.72	250	−0.265 (10.3)
Reorganisation energy λ = 0.65 eV			
	138	14.4	−0.120 (4.65)
	83.4	49.7	−0.165 (6.39)
	32.1	920	−0.265 (10.3)
Reorganisation energy λ = 0.8 eV			
	390	40.7	−0.120 (4.65)
	230	137	−0.165 (6.39)
	80.9	2321	−0.265 (10.3)

The rates of forward and backwards electron transfer between the iron–sulfur clusters F_X and A_{1B} computed for a few values of redox midpoint potential that span the range reported in the literature and for different values of the reorganisation energy λ are shown. The backward rate of electron transfer are weighted according to the Boltzmann distribution.

dependent on the rate of F_X reoxidation. This is agreement with experimental observations relating to the effect of point mutations in the protein surrounding F_X. In *C. reinhardtii* membrane preparations of a site directed mutation of an aspartate residue close to the cysteine ligand of the iron–suphur cluster to a leucine (PsaA-D576L), the decay of the spin-polarised electron spin echo arising from $[P_{700}^{+}A_1^{-}]$ was found to be almost two-fold slower than that observed in the wild-type [170].

However, independently of the exact rate value assumed, both radical pairs $[P_{700}^{+}A_1^{-}]$ and $[P_{700}^{+}F_X^{-}]$ would display a similar first moment of the population distribution and therefore decay on closely related timescales. The strong dependence of the decay of A_1 on the rate of F_X reoxidation indicates that this is a crucial factor in the overall electron transfer calculation, as it is the F_X to F_A electron transfer step, which provides the driving force for the overall electron transfer because of the almost isoergentic potential of $A_{1(A/B)}$ and F_X.

3.2.3. Discussion of alternative kinetic models

3.2.3.1. Monodirectional electron transfer along the PsaA reaction centre subunit: distribution of the cofactor redox potential. In the previous paragraphs, a model has been presented that, within the limits of accuracy of the estimates of electron tunnelling parameters, can provide a sufficiently detailed description of the reoxidation kinetics of the phylloquinone A_1 assuming a bi-directional electron transfer chain. It should be noted that although most of the experimental observations are satisfactorily described, there are a few experimental results which can argue against some of the original assumptions employed in the kinetic modelling. Primarily, the functionality of the PsaB bound branch has been disputed [37,48,49,51,57,58,60–62,163,171]. In view of the site directed mutational experiments, the involvement of both the A_1 phylloquinones appears as the most straightforward explanation, although a bias of the redox potential of either the A_{1A} phylloquinone or the iron–sulfur centre F_X induced by the mutation of the PsaB subunit can, in principle, explain the effect of decay lifetimes.

If that were the case, the simplest explanation to describe the experimentally accessible lifetimes and the temperature dependence of the A_1 reoxidation kinetics would be to assume a rather large distribution of the A_1 (or F_X) redox potential midpoint, which would, in turn, result in an almost continuous distribution of forward (and backwards) rate constants [172–174]. A distribution of redox potential can be thought of as the result of the cofactor interaction with a slightly different conformational state of the reaction centre proteins [172–174]. A possible distribution of redox potentials of the iron–sulfur clusters F_X, F_A, and F_B, as well as of the phylloquinone A_1, has been originally suggested by Brettel [19] to explain the heterogeneity of

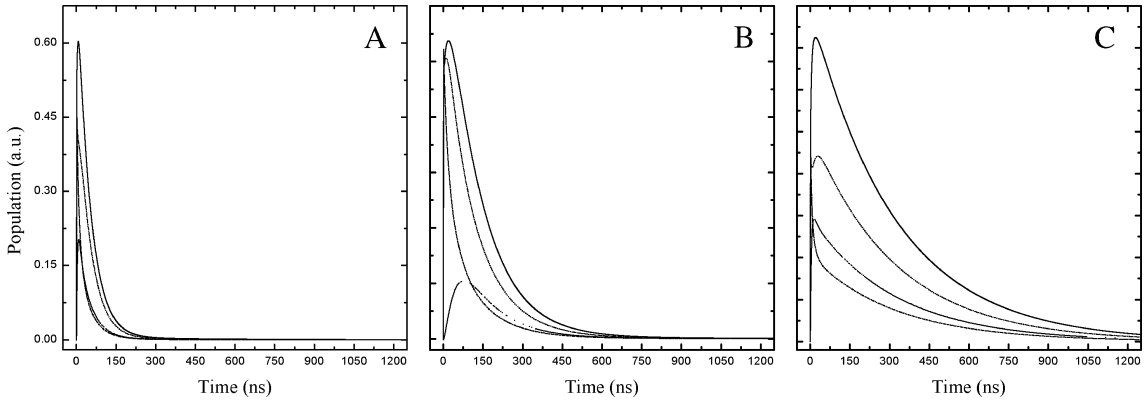

Fig. 8. The effect of altering the reoxidaton rate of F_X on the population evolution of the radical pairs $[P_{700}^{+}A_1^{-}]$ (solid lines), $[P_{700}^{+}A_{1A}^{-}]$ (dashed lines), $[P_{700}^{+}A_{1B}^{-}]$ (dash-dotted lines), and $[P_{700}^{+}F_X^{-}]$ (dotted lines). The electron transfer simulations were performed for three representative values of F_X reoxidation rate: $k_{FX\rightarrow FA}(10\ ns)^{-1}$ (A); $k_{FX\rightarrow FA}\ (47\ ns)^{-1}$ (B); $k_{FX\rightarrow FA}\ (90\ ns)^{-1}$ (C). The different values of the F_X reoxidation rate constants were obtained by varying the value of λ, so that the equilibrium constants between A_{1A}, A_{1B}, and F_X and F_X and F_A are not altered.

the electron transfer reaction in PS I at cryogenic temperatures [19,53]. In the case of a redox potential distribution, the decay kinetic will not be essentially exponential but described by an analytic function in the form of:

$$F(t) = \int_0^\infty P(\tau)\cdot e^{-\frac{t}{\tau}}\cdot \mathrm{d}u \qquad (10)$$

where $P(\tau)$ is the normalised distribution of lifetime [175,176].

An analysis of the phylloquinone reoxidation kinetics in terms of lifetime distributions has not yet been attempted. Preliminary model calculations indicate, in order to mimic the effect of site directed mutants on the A_1 reoxidation decay, and assuming a Gaussian distribution of the A_1 redox potentials, the mean phylloquinone E_m value would be set at about that of F_X and the width of the distribution (FWHM) would be as wide as ~100 mV (data not presented). This value is not dissimilar from the width in the energy distribution of about 118 mV (FWHM) estimated for the primary donor of bacterial reaction centre [177]. It should be expected that when a possible distribution of the E_m value of F_X is taken into consideration, the variance of A_1 redox potential distribution should narrow to a significant extent. Therefore, in our opinion, the width of the potential distribution employed in these preliminary calculations should be considered as an upper limit.

3.2.3.2. The effect of collapsing the ionic transmembrane potential on the kinetics of the $[P^+_{700}A^-_1]$ and $[P^+_{700}F^-_X]$ electron transfer reactions. Whatever the case, it is apparent that in the model calculation of electron transfer in PS I based on electron tunnelling presented in this study, a quasi-equilibrium scenario at the level of the A_1 to F_X electron transfer step is attained, as originally proposed by Brettel and Setif [59]. This model has been questioned in Ref. [36].

The photosystems in the natural environment, the photosynthetic membrane, are subjected to the electric part of the electrochemical potential [178]. Therefore, the total free energy for any of the electron transfer reaction would not only be dependent on the ΔG^0 but also on the field applied across the thylakoid membrane. The absence of any effect on the kinetics of phyloquinone reoxidation upon collapsing the electrochemical potential by about ~50 mV was reported by Joliot and Joliot and taken as an evidence of large driving force for A_1 reoxidation reactions [36]. Although 50 mV is a significant difference, the relevant quantity which would affect the free energy of any electron transfer reaction is the local field at the level of the donor and acceptor molecules. In a first approximation, this can be estimated by dialectical weighting. Joliot and Joliot [36] suggested a difference of about 10 mV in the applied electric field in the presence or absence of transmembrane potential. In their measurements, they observed only minor differences in the kinetics in these cases, with lifetimes of 19 ns, 172 ns, and 461 ns, in the absence, and 18 ns, 168 ns, and 311 ns, in the presence of the transmembrane field. We have performed model simulations in which a similar difference in free energy for the reoxidation kinetics of A_1, F_X, and F_A has been considered. The results are presented in Fig. 9. In the model simulations, the calculated lifetimes shifts from 4.5, 15, 172, and 199 ns, without any externally applied electric field to 3.8, 16, 182 and 223 ns, when a field equivalent to potential of 10 mV is considered.

Although the differences in the simulations of A_1 reoxidation in the presence or absence of an external electric field appear to be smaller than those previously simulated [36], the relatively larger effect of $\Delta\psi$ on the long-lived lifetimes component, which was observed in the measurements, is qualitatively reproduced. There appear to be differences in the kinetics of A_1 reoxidation which are outside the signal-to-noise ratio in the measurements and should therefore be detected.

It is also interesting to notice that Witt and coworkers [178–181] have shown a linear dependence of the electrochromic signal associated with the vectorial charge translocation across the thylakoid membrane to the field intensity. The theory predicts a quadric response for molecules which have an inducible dipole moment. These results can be understood if the change of electric field associated with the photosystem photochemical reaction and coupled ion transport is overlapped to a stable ion field which is at least an order of magnitude larger [178,181]. It has been suggested that such a field might be created by charged phospholipids in

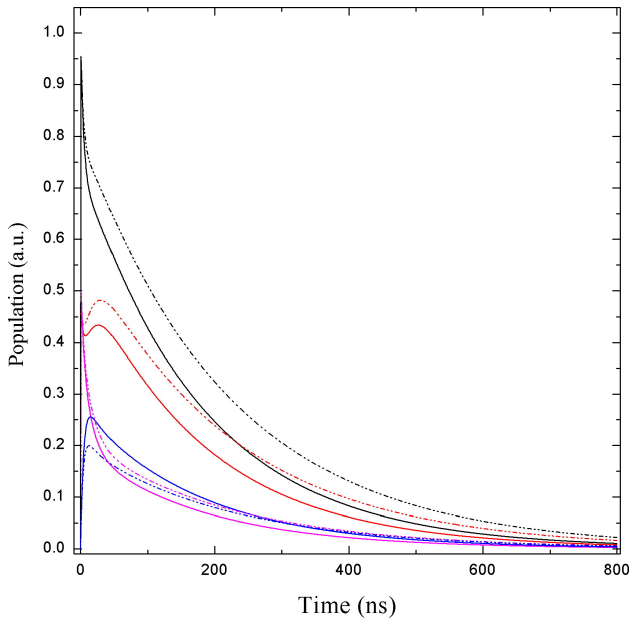

Fig. 9. The effect of applying an external electric field potential on the population evolution of the radical pairs $[P^+_{700}A^-_1]$ (black lines), $[P^+_{700}A^-_{1A}]$ (red lines), $[P^+_{700}A^-_{1B}]$ (magenta lines), and $[P^+_{700}F^-_X]$ (blue lines). The relevant lifetimes are: 4.5 ns, 15 ns, 172 ns, and 199 ns, without applied electric field (solid lines); and 3.8 ns, 16 ns, 182 ns, and 223 ns, with an applied field equivalent to potential of 10 mV (dash dotted lines).

the thylakoid membrane [181]. In this case, the kinetics of A_1 reoxidation, but in general, of all the electron transfer reaction, are expected to be significantly different when monitored in the membrane or in isolated Photosystem I particles. However, they are, in general, quite consistent. In contrast to an isomorphous dielectric, proteins have a well-defined arrangement of residues; therefore, polar and charged groups have a reduced degree of freedom of rearrangement when an external electric field is applied. Moreover, the dielectric relaxation properties can vary significantly amongst different regions of the protein [182,183]. Reasons for the discrepancy between the quasi-equilibrium model of A_1 reoxidation and the effect of collapsing the electrochemical potential across the thylakoid membrane [36] could probably be due to the difficulties of having a precise estimate of the electric field in the region of membrane that bounds the electron transfer cofactors.

3.2.3.3. Asymmetry in the value of the reorganisation energy from the phylloquinones bound to the PsaA and the PsaB reaction centre subunits. In the frame of the bi-directional electron transfer model, the structural data indicates that the edge-to-edge distances between the two phylloquinones and F_X are essentially the same [3,46]. Therefore, the only way to describe two substantially irreversible ($\Delta G^0 \ll 0$) electron transfer reactions is to assume a rather large difference in the reorganisation energy on the two electron transfer branches. Assuming the same free energy of about −60 meV, equivalent to an equilibrium constant Keq of about 0.1, and in order to obtain forward electron transfer rates of ~15 ns and ~150 ns for A_1 reoxidation on the PsaB and PsaA branches [19,36,38,47,59,157], values of the reorganisation energy λ of 0.75 eV and 1.1 eV should be assumed, respectively, as also previously discussed by Agalov and Brettel [38]. As the decay lifetimes are not always straightforwardly correlated with the forward electron transfer rates, we have performed kinetic simulations of this scenario using the same system of coupled differential equation described in Section 2.2, and the results are presented in Fig. 10. The resulting decay lifetimes in the nanosecond range obtained from the electron transfer kinetic simulations are 13.8 ns and 169 ns and are almost equally weighted. The first moment of the decay distribution for the $[P^+_{700}A^-_1]$ radical pair is 155 ns. The $[P^+_{700}A^-_{1A}]$ radical pair, when the picosecond components not detected in the measurements are ignored, essentially decays mono-exponentially with a lifetime of 169 ns. The $[P^+_{700}A^-_{1B}]$ radical pair decay is dominated by the 13.8 ns lifetime. The decay of the $[P^+_{700}F^-_X]$ radical pair exhibits a first moment of the decay distribution of 152 ns, which is close to the decay of the $[P^+_{700}A^-_1]$ and the $[P^+_{700}A^-_{1A}]$ radical pairs, although the rise time of $[P^+_{700}F^-_X]$ is slowed down to about 14 ns, compared to the about 4.5 ns simulated previously.

It is therefore apparent that the assumption of a different reorganisation energy for the reoxidation of the A_{1A} and the A_{1B} phyllosemiquinones can provide a straightforward description of the observed biphasic kinetics and of the effect of site directed mutations in the surroundings of the quinones on each electron transfer branch. There are, however, several observations which make us skeptical about this hypothesis. Firstly, a difference in the reorganisation energy of about 350 meV between the two electron transfer branches appears, in our view, quite inconsistent with the similarity in the quinone binding sites revealed by the electron transfer structures [3,46]. Differences in the strength of hydrogen bonding of the phylloquinone might [70,184,185] be at the origin of the proposed asymmetry in the redox midpoint potential, as the latter would be dependent on the extent of the ionic state as stabilised by the surroundings, and in the reorganisation energies as well. However, while the difference in redox midpoint potential suggested in the present study is in an interval of 10 to 40 mV, equivalent to free energies of 10–40 meV, at least a ten times larger difference between the proposed values of λ should be postulated to describe the kinetics of A_1 reoxidation.

Furthermore, the heterogeneity of electron transfer in PS I at low temperature [19,53] and the observation that one phylloquinone molecule (A_{1A}) is more readily photoaccumulated than the other [20,62,158,184] are not promptly understandable if the electron transfer reaction from both phylloquinones were thermodynamically favourable. This fits much better in a scenario in which the two phylloquinones posses a different redox potential, one of the two possibly more positive then F_X, as discussed previously.

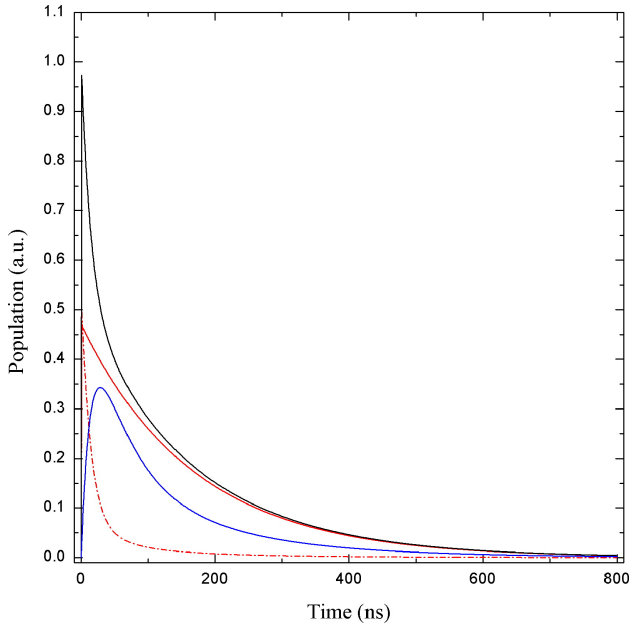

Fig. 10. Population evolution of the secondary radical pairs $[P^+_{700}A^-_{1A}]$ (red, solid line), $[P^+_{700}A^-_{1B}]$ (red, dash-dotted line), and $[P^+_{700}F^-_X]$ (blue, solid line), calculated for ΔG^0 values of 60 meV on both electron transfer branches and reorganisation energies of 0.7 eV and 1 eV for the PsaB- and the PsaA-bound phylloquinone reoxidation reactions. The decay of the $[P^+_{700}A^-_1]$ radical pair (back solid line) is also presented. The relevant lifetimes are: 13.8 ns, 169 ns, and 191 ns.

3.2.3.4. A possible role for TrpB679 as an electron transfer intermediate. Finally, it is of interest to mention a different electron transfer model proposed by Ivashin and Larsson [92] that postulated the involvement of tryptophan (TrpB673 in *S. elongatus*) as a possible intermediate between the phylloquinones and F_X. This Trp is located at an edge-to-edge distance of 4.2 Å from the A_{1B}, 6.56 Å from A_{1A}, and 4.6 Å from F_X [3]. It is clear from the basic theory for electron transfer tunnelling discussed in Section 2 that the shorter distance between this tryptophan residue and A_{1B} would make the rate of electron transfer faster compared to the one from the A_{1A} quinone. In fact, the calculated electron coupling energies for the TrpB673–A_{1A} and the TrpB673–A_{1B} couples have values of 6.2 cm^{-1} and 0.15 cm^{-1} [92]. From the Marcus equation and assuming the same values for the free and reorganisation energies, the rate of reoxidation of A_{1B} should be about 40 times faster than that of A_{1A}. The value of the electronic coupling between the A_{1A} and F_X is 0.28 cm^{-1}, higher than the one estimated for A_{1A} TrpB673. It was therefore proposed that TrpB673 can act as an electron transfer intermediate between A_{1B} and F_X, while A_{1A} would reduce F_X directly. Even though this is an attractive hypothesis, there are no reports in the literature of a direct observation of a Trp anion involved in biological electron transport. In fact, the redox midpoint potential for the Trp/Trp^- should be almost as negative as the one determined for Tyrosine, which is about −1 eV, i.e., almost isoenergetic with the primary acceptor/donor. This, in turn, would make the reaction extremely endergonic. As a consequence, even at room temperature, and in optimal conditions of $\Delta G \approx -\lambda$, the back reaction would be orders of magnitude faster, as it is governed by the Boltzmann distribution. Therefore, we consider the proposal that TrpB673 is involved as an 'proper' ET intermediate as unlikely, although the involvement of this residue in electron transfer taking place by the superexchange mechanism should be taken into consideration [92].

In summary, we have, in this section, considered different approaches and possible explanations to describe the experimental observations of the kinetics of phylloquinone A_1 reoxidation. We, at present, favour a model in which the differences in observed reoxidation rates are associated with an asymmetry in the redox midpoint potential and, therefore, of the driving force in the reoxidation reaction. The redox potential of the A_{1A} is estimated to be 10 to 40 mV more positive than the one of the A_{1B}, both of them being almost isoenergetic with the iron–sulfur centre F_X. This is a proposition first advanced by Brettel and coworkers [19,59] for the A_{1A} quinone, but which is now extended to both the electron transfer branches. We favour a scenario in which the redox potential of A_{1A} is more positive than the one of F_X. This reaction would be therefore slightly thermodynamically less favourable, explaining the observation that about 40–50% of PS I reaction centres are incapable of reducing F_X at temperatures lower than about 150 K [53] when the uphill energy gap cannot be overcome by the thermal energy of the environment. On the other hand, the redox potential of A_{1B} is considered as more negative than F_X; therefore, both the faster forward rate and the ability of the remaining fraction of PS I centres to reduce F_X at low temperature can be explained in this context. Due to the coupling of electron transfer reactions and the relative 'shallow' equilibrium between the different redox centres, the observed decay lifetimes do not necessarily reflect the rate of forward electron transfer. This is a general consideration which has been often overlooked in the analysis of reduction–oxidation kinetics of multi-centre redox systems. Finally, it is also generally observed that the decay of the $[P^+_{700}F^-_X]$ and the $[P^+_{700}A^-_1]$ radical pair takes place in the same time window, independently of the precise kinetic model adopted, providing an explanation for the fact that F_X is usually not observed as a kinetic intermediate. Therefore, the original interpretation that the rate of F_A reduction by F_X should be faster than F_X reduction is not necessarily correct, taking the present model calculations in consideration.

3.3. Reactions in the microstime range: reduction of the iron–sulfur clusters, and the equilibrium between F_A and F_B

Finally, in order to provide a complete description of the electron transfer events in the PS I reaction centre, we are going to discuss the reactions involving the iron–sulfur centres F_A and F_B, which are usually monitored, as they are reduced by low temperature (below 70 K) illumination of PS I [24,25,27,28,30,40,41,74,158]. This was the first evidence that the two clusters might have a similar redox potential, and that the charge was significantly shared between them [24,25,27,28,30,40,41,74,158]. The redox potentials of F_A and F_B have been estimated either by potentiometric titration in combination with low temperature EPR, or by the optically monitored titration of the recombination kinetics of the $[P^+_{700}FA^-]$ and the $[P^+_{700}F^-_B]$ radical pairs, and shown to lie in the −450 to −590 mV region [25,29,40,74,169]. In both cases, F_B is estimated to have a more negative potential compared to F_A; therefore, this reaction is endergonic. It is generally accepted that, based on the rate of ferredoxin (Fd) reduction by the whole PS I electron transfer chain, which is about 500 ns [45,60,186,187], electron transfer in between the three Fe–S centres should be faster than, or on the same time scale as, Fd reduction. The energy gap between the F_A and F_B centres is in the range of 20 to 60 mV [19,25,29,40,74,79,169]. The electron transfer between F_A and F_B has also been investigated in a recombinant, isolated PsaC subunit, which binds both centres [42–44], but no electron transfer can be detected [188,189]. However, rates of about 300 ns were measured in analogous bacterial ferredoxins [190 191]. There is, to our knowledge, no direct estimate of the rate of electron transfer between F_A and F_B. A rate of about 300 ns can be simulated by a simple tunnelling rate equation expression, assuming a ΔG value of 30 meV and a reorganisation energy of 1 eV. Although this is a value for

the reorganisation energy which is in the range often reported for electron transfer proteins, it is a slightly higher estimate compared to the values used for the other electron transfer reaction in PS I in this study, but it is consistent with the work by Sigridson and coworkers, which has estimated an even higher value of λ for Fe–S compared to a variety of cytochromes [192].

The rate of F_B reoxidation, monitored as Fd reduction, has been shown to be multiphasic, with estimated lifetimes in the order of ~0.5/1 μs and ~20/80 μs [45,186,187,193]. The most straightforward interpretation of polyphasic reduction of Fd is obtained when the fast phase is associated with a tightly bound Fd population and slow phase is thought to be limited by the diffusion of the soluble electron carrier and, hence, reflects the binding rates of Fd to the stromal docking site of Photosystem I [45,186,187,193]. These aspects have been discussed extensively in a recent review by Setif [45]. Since the main purpose of this study is investigating the electron transfer reactions within the PS I reaction transfer complex, we have limited our simulations to the tightly bound Fd pool and neglected the second-order diffusional process.

The results of simulations of the electron transfer in PS I for the radical pair couples $[P^+_{700}F^-_X]$, $[P^+_{700}F^-_A]$, and $[P^+_{700}F^-_B]$ are presented in Fig. 11. The rise time of the radical pair $[P^+_{700}F^-_A]$ is 172 ns, which matches the decay of $[P^+_{700}F^-_X]$, while the $[P^+_{700}F^-_B]$ radical pair exhibits a rise time of 199 ns. At this point it, is interesting to compare the rise times obtained from model calculations for all the radical pairs investigated with experimental data available from either photovoltage or electrochromic effect measurements. The

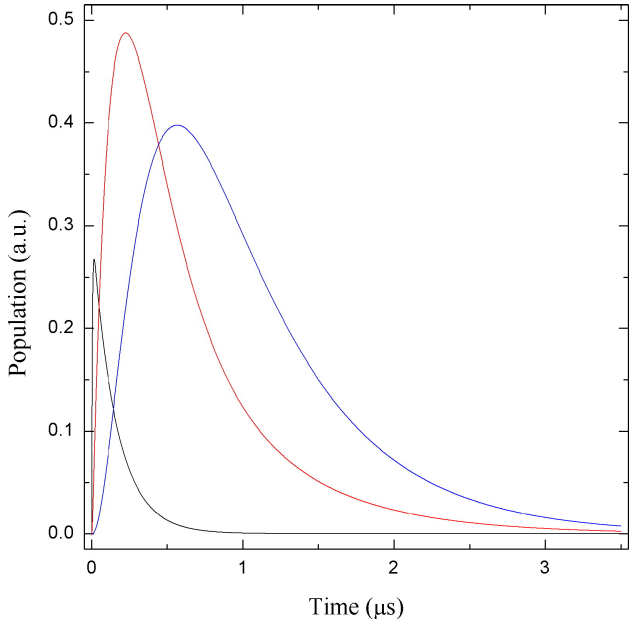

Fig. 11. Population evolution of the radical pairs $[P^+_{700}F^-_X]$ (black line), $[P^+_{700}F^-_A]$ (red line), and $[P^+_{700}F^-_B]$ (blue line), calculated using the ΔG^0 values of −155 meV and +30 meV for the $[P^+_{700}F^-_X]$ and the $[P^+_{700}F^-_A]$ reoxidation reaction, respectively.

fast photovoltage measurements will resolve the initial rise of the $[P^+_{700}A^-_1]$ radical pair, but due to instrumental limitation, the time window between several hundred of picoseconds and a few nanoseconds is not covered by this technique. Electrochromic measurements do not have a picosecond temporal resolution but have the advantage that nanosecond resolution can be achieved without the need for deconvolution and correction for the diffusional relaxation of the potential during the measurements. Both the techniques, which monitor electrogenic reactions in the system, detect a rise phase shorter that 5–7 ns, which is instrument limited [36,149,174,194] and which has been essentially assigned to A_1 reduction by A_0. This initial fast rise phase probably includes the contribution of the $[P^+_{700}A^-_{1A}]$ and $[P^+_{700}A^-_{1B}]$ radical pair couples and might reflect some contribution from the $[P^+_{700}F^-_X]$ radical pair, which would have a minor importance due to the relatively low population of this electron transfer intermediate, and the dependence of the signal on the dielectrically weighted distance. The first phase resolved by photovoltage in the nanosecond time window has a lifetime of about 150 ns that was interpreted as the reduction of F_X and $F_{A/B}$ [149,194]. The tunnelling simulations of electron transfer for the iron–sulfur clusters are in fair agreement with these measurements since a main rise component of about ~170 ns is estimated for F_A reduction. Similarly, the 199 ns rise time for the $[P^+_{700}F^-_B]$ radical pair matches a minor electrogenic phase of ~200 ns detected by both photovoltage [149,194] and electrochromic bandshifts [36], which was also interpreted as reflecting electron transfer between the two terminal Fe–S centres F_A and F_B. The small electrogenic amplitude of the 200 ns phase can be understood if one considers the location of the terminal Fe–S cluster revealed by the X-ray structure of PS I from *S. elongatus* [3]. The projection of the distance between the F_A and F_B centres on the membrane plane is small, as the two clusters appear to be located almost parallel, forming an angle of ~30° between the axes which crosses the cluster and the plane perpendicular to the membrane plane. The simulation results in an average decay lifetime of 272 ns for $[P^+_{700}F^-_A]$ and 274 ns for $[P^+_{700}F^-_B]$. The latter values mirror the rate of Fd reduction [45,186,187]. The weighted average decay lifetime parameter describes how fast the radical pair is populated. When the rate of population and decay of the state falls in a similar time scale, as it is the case for the iron–sulfur centres, the use of the first moment of the distribution is a more useful and intuitive parameter, as it is directly reflecting the apparent $\tau_{1/2}$ of the radical pair decay. Values of 800 ns and 1.1 μs are obtained, in this case, for the $[P^+_{700}F^-_A]$ and the $[P^+_{700}F^-_B]$ radical pairs, respectively. The 1.1 μs decay lifetime estimated for the F_A and F_B reoxidation closely matches the observed decay of the spin-polarised EPR signal [33,57,195], detected at room temperature and associated with the $[P^+_{700}Fe–S^-]$ centre. Due to very fast magnetic relaxation in the iron–sulfur centres, the coherence in the acceptor partner in the spin-

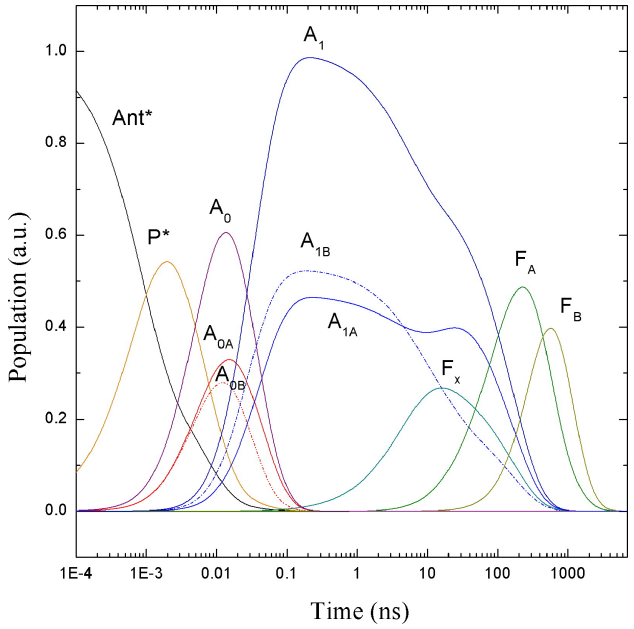

Fig. 12. Population evolution of all the radical pairs involved in electron transfer reactions, presented on logarithmic time scale in order to illustrate the pico- to micro-second time range investigated. The electron transfer simulation in which only the unambiguously spectroscopically detected electron transfer intermediates are considered.

correlated radical pair is lost; therefore, it is almost impossible to associate the observed signal with any particular iron–sulfur cluster, but the decay of the net magnetisation associated with the P^{+}_{700} donor can still be observed (see review by van der Est [195]). In the frame of the tunnelling simulations presented here, we suggest that the observed decay reflects the $[P^{+}_{700}F^{-}_{A/B}]$ radical pairs rather than $[P^{+}_{700}F^{-}_{X}]$.

In Fig. 12, the dynamics associated with all the electron transfer processes considered in these electron tunnelling simulations are presented on a logarithmic time scale in order to cover the almost ten orders of magnitude of decay rates investigated, thus providing a complete picture of electron transfer in the PS I reaction centre.

4. A revisited energetic scheme of electron transfer cofactors in PS I

In the previous sections of this review, the electron transfer reactions and their relation to electron tunnelling parameters have been discussed. On this basis, it has been possible to derive a scheme for the free energy of the electron transfer cofactors, as this is one of the parameters which influence the forward, and backward, electron transfer rates. The difference in redox potential between donor and acceptor can be derived based on simple thermodynamic considerations as well. It should be noted that, in general, the estimate of redox potential from free energy should be considered only as an approximation, as electrostatic interaction between closely spaced intermediates is generally neglected. The influence of electrostatic interaction on the estimate redox potential is extensively discussed by Brettel [19], who first derived a putative complete energetic scheme for PS I. In the following, the original suggestions of Brettel [19] are revised in the view of recent reports in the literature and their interpretation above in the frame of bi-directional electron transfer model.

The free energy of the primary donor excited state can be derived from its photon absorption. Although some species-specific difference have been reported [196], the minimum of the $[P^{+}_{700}-P_{700}]$ absorption difference at about 700 nm can be considered as a reasonable approximation as the peak absorption of the primary donor [4,5]. A free energy of 1.78 eV is obtained in this case. Thermodynamic consideration leads to the conclusion that only about 70–80% of the free energy is available for electron transfer events [197–200] because of entropic losses, which would result in an estimate of redox potential for the primary donor of about 1.3 eV.[1]

Based on the radical pair equilibrium, a drop of 65 meV between P_{700} and the primary acceptor is determined. This is a smaller energy gap than the one estimated between A_0 and P_{700} by means of delayed luminescence, which is in the range 140–250 meV [94–96,150]. In order to accommodate this difference, a possible involvement of the accessory Chl in electron transfer events should be considered. Otherwise, the 65 meV should reflect the free energy between the "unrelaxed" primary acceptor and donor while 140–150 meV should reflect the difference between the "relaxed" primary acceptor and donor. Since there are not, in our view, at present, any unequivocal experimental support for either of the two cases, we will present two alternative schemes in which either A_0 or Chl_{acc} is considered as putative primary electron acceptors.

The free energy difference between A_0 and A_1 can be estimated from the forward electron transfer rates, which has been estimated as 26 ns^{-1} and 46 ns^{-1} for the PsaA and the PsaB electron transfer branches, respectively (Figs. 1 and 2). The free energy for this electron transfer step can be obtained by back estimation from the electron transfer rate, assuming a certain value for the reorganisation energy. It should be noted that in the latter case, it involves the solution of quadratic equations; therefore, two possible redox potentials for A_0 will be estimated.

In the models which consider A_0 as the primary acceptor, the free energy of A_0 should be reconciled with that obtained from the reversible radical pair equilibrium (−1715 meV). The rates of A_1 reduction on the PsaA and

[1] Although the concept of entropy losses quantifiable by the thermodynamic efficiency of the Carnot cycle is a widely accepted concept, it is worth noticing that Yourgrau and van der Merwe [201] and successively Parson [202] have questioned this view. In these studies it is suggested that the Gibbs free energy is essentially equal to the total free energy ($\Delta G^0=\Delta U=h\nu$). In this case the redox potential of the primary donor excited state could be as high as −1.8 eV.

the PsaB reaction centre subunits are described in the frame of tunnelling of electron transfer by free energies of −550 and −570 meV and reorganisation energies of 0.4 and 0.46 eV, respectively. Taking into consideration the proposed 'quasi-equilibrium' between the two phylloquinones and F_X and assuming the same free energy for A_0 on both electron transfer branches, the free energy of F_X is then poised to ~ −1150 meV. Similar results can be achieved when the activation energies on the two branches are set to 0.83 eV and 0.67 eV. However, because of the similarities of the cofactor binding sites on both the reaction centre subunits, a difference in the reorganisation energy of about 150 meV appears unlikely. The estimated free energy of the A_{1A} and the A_{1B} quinone is then −1140 meV and −1162 meV, respectively. These free energies can be associated with a redox midpoint potential of about −690 mV for the iron–sulfur centre F_X, and ~ −700 mV and −678 mV for the A_{1B} and A_{1A} phylloquinones, respectively. The value for F_X falls in the average of the data reported in the literature [75–77]. However, redox potentials as negative as −730 mV have been suggested for this electron transfer intermediate [77]. These values can be reproduced if slightly different reorganisation energies are assumed. For example, letting the value of λ be 0.37 (0.79) and 0.43 (0.63) for A_0 reoxidation on the PsaA and the PsaB branches, respectively, this will, in turn, lead to an estimate of the F_X redox midpoint potential of ~ −720 mV in the upper negative range of the values reported in the literature.

Independently from the precise value of the reorganisation energy estimation, and the assumed free energy difference for A_0 reduction, it is apparent that A_1 reduction is driven by a free energy difference in the 300–500 meV range and is therefore substantially irreversible. The estimates in free energies are consistent with redox midpoint potential of about −530 mV for F_A, −560 mV for F_B, −690 mV for F_X, and ~ −700 mV and −678 mV for A_{1B} and A_{1A} phylloquinones, respectively. The complete set of redox potential estimates are presented in Fig. 13 and are also reported in Table 3, where they are compared with some of the values previously determined indirectly by analysis of charge–recombination reactions and delayed luminescence studies.

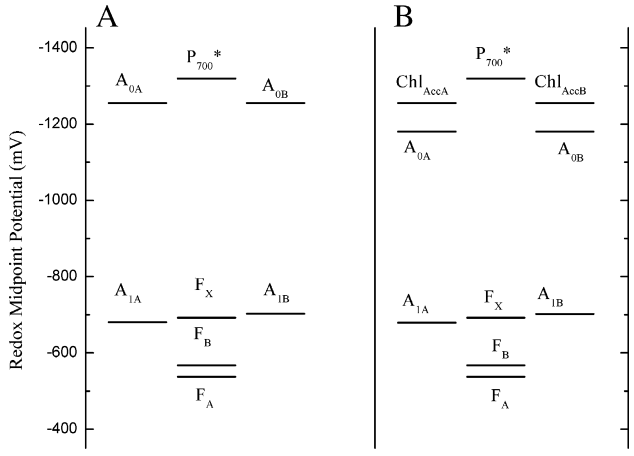

Fig. 13. Energetic properties of electron transfer cofactor in PS I derived from the analysis of kinetic transients in terms of Marcus theory of tunnelling for electron transfer reactions ignoring (A) or considering (B) the accessory chlorophyll as possible electron transfer intermediates.

From the overall energetics of the system, it should be noted that the main driving force for the whole electron transfer in PS I is associated with the reduction of A_1 by A_0 (on both electron transfer routes on PsaA and PsaB), the reduction of F_A by F_X, and the reduction of the soluble carrier Fd by F_B. The other electron transfer steps are associated with a rather small driving force, which is even more accentuated in the case of oxidation of A_1 by F_X and F_A by F_B, reactions which are considered to be endergonic and take place against a driving force of about 5/20 meV. In the case of long-lived radical pairs, back reactions can take place and eventually populate the potentially harmful Chl triplet state of the primary donor [19,34,65,144–146]. This can then interact with molecular oxygen generating

Table 3
Electron transfer tunnelling parameter of PS I redox cofactors

ET intermediate	E_m (mV)	X_{ij} (Å)	λ (eV)	k_f (ns^{-1})	k_b (ns^{-1})	τ^r_{av} (p/ns)[a]	τ^d_{av} (p/ns)[a]	$\bar{\tau}$ (ns)	E^b_m (mV)
P^*_{700}	−1320	–		100[c]	8.3	0.79[a]	8.5[a]	0.00234	
A_{0A}/A^-_{0A}	−1280	9.7	0.4	26	$<10^{-9}$	8.9[a]	32.6[a]	0.231	~ −1050
A_{0B}/A^-_{0B}	−1228	9.8	0.46	48	$<10^{-9}$	6.5[a]	21.0[a]	0.118	n.d.
A_{1A}/A^-_{1A}	−671	6.5	0.62	0.046	0.084	35.5[a]	114	200	−820, −810, −740 −696, −596
A_{1B}/A^-_{1B}	−696	6.4	0.62	0.082	0.055	24.9[a]	51.7	178	−696
F_X/F^-_X	−680	8.9[d]	0.55	0.021	4.7×10^{-5}	4.7	155.1	199	−730, −705, −670, −650
F_A/F^-_A	−526	11.6	1	0.0035	0.0011	172.1	272.9	800	−540, −520, −590
F_B/F^-_B	−556	9.5	n.d.	0.002	n.d.	199.6	274.7	1126	−590, −570, −540

Compilation of the parameters using in the electron transfer simulation, E_m is the redox midpoint potential (values taken from the literature are reported for better comparison), X_{ij} is the edge-to-edge distance, λ is the reorganisation energy, and k_f and k_b are the rate of forward and backward electron transfer, respectively. Also listed are the main kinetic parameters derived for each electron transfer intermediates, τ^r_{av} is the rise average lifetime, τ^d_{av} is the decay averaged lifetime, and $\bar{\tau}$ is the fist moment of the decay.

[a] Units are ps.

[b] Values taken from the literature, n.d. not determined.

[c] Rate of charge separation on each electron transfer branch.

[d] Due to uncertainty about the spin distribution over the two quinone molecule, the same edge-to-edge to F_X has been assumed.

the extremely reactive singlet oxygen species. In the case of the $[P_{700}^{+}F_{A/B}^{-}]$ radical pair state, the recombination reaction rate has been estimated to be about 20 to 100 ms [39,76,160,168] and, therefore, is unlikely to be a significant competitor of forward electron transfer in conditions when Fd or any exogenous diffusible electron acceptor is present. Moreover, due to the very fast relaxation within the Fe–S clusters, electron spin coherence is severely decreased or lost, making the recombination reaction to the triplet state an extremely unlikely process. Similar considerations can be raised in the case of the $[P_{700}^{+}A_{1(A/B)}^{-}]$ radical pairs. In fact, electron transfer from A_{1B} to F_X would occur in the tens of nanosecond time scale, much faster than the estimated recombination kinetics on this branch, which has been estimated in the range of 3 to 15 μs. On the other hand, the $[P_{700}^{+}A_{1A}^{-}]$ population has a lifetime of about 200 ns, which is long enough to promote charge recombination [34,39,76,160,168]. However, it should be noted that, in this model, due to the equilibrium between A_1 and F_X, a significant loss of correlation is expected in this case, which would, as described above, strongly diminish the chances of recombination to the triplet state.

5. Conclusions

The electron transfer reactions within Photosystem I has been analysed in terms of Marcus theory for electron transfer tunnelling, assuming a bi-directional electron transfer kinetic model in which the equilibrium between the two tightly bound phylloquinones and the iron–sulfur cluster F_X, and, generally, in between all the electron transfer steps, is taken into consideration. Essentially, all the electron transfer rates reported in the literature can be described, ranging from the picosecond timescale reactions associated with primary charge separation to the reduction of the terminal iron–sulfur centres, which occurs on the microsecond timescale. The energetics for all the bound cofactors can be derived from this analysis and shown to agree well with most of the reported estimates, obtained either by direct redox titration or indirect estimates from spectroscopic measurements. An exception to this general behaviour is the redox potentials estimated for the $[P_{700}^{+}A_{1A}]/[P_{700}^{+}A_{1A}^{-}]$ and $[P_{700}^{+}A_{1B}]/[P_{700}^{+}A_{1B}^{-}]$ radical couples for which a potential of about −670 and −695 mV is estimated, while the redox potential of F_X is estimated at −680 mV. We suggest that both quinones are substantially isoenergetic with respect to F_X. Because of the uphill electron transfer from A_1 to F_X on the PsaA side branch against a free energy of 0.015 eV compared to a downhill electron transfer with a favourable driving force of 0.01 eV on the PsaB branch, a difference of almost one order of magnitude in the apparent rate constants associated with the two electron transfer steps is observed, while the intrinsic rate constant is rather similar.

Notably, the only reactions which are virtually irreversible, because of rather larger driving forces, are the ones associated with the reduction of A_1 and F_A, but the possibly deleterious recombination reactions to the donor triplet state are minimised because of significant loss of correlation in the spin coupled radical pairs due to the fast magnetic relaxation of the iron–sulfur centres.

Acknowledgements

This work was supported by grants from the U.K. Biotechnology and Biological Sciences Research Council (BBSRC) (CO0350,CO7809, and B18658) and the European Union TMR programme (Contract No. FMRX-CT98-0214). We are thankful to Drs. L.P. Dutton and C.C. Moser (Penn State University), Th. Renger (Freie University, Berlin), E. Shlodder (Techishe University, Berlin), E. Bordignon, and D. Carbonera (University of Padoa) for providing us with material before publication, and to Dr. R.C. Jennings, A.P. Casazza, and G. Zucchelli (University of Milan), A.R. Holzwarth (Max Plank Institute, Mulheim), F. Rapaport, and M. Byrdin (IBPC, Paris), I Kuprov (University of Oxford), S. Larson (Chalmers), and S.E.J. Rigby (Queen Mary, London) for stimulating discussion. We also wish to express gratitude to Dr. A. Cuff and Ms. F. O'Boyle (Queen Mary, London) for helping in the analysis of the crystallographic structure, and Drs. C.D. Syme and H.K. Leech for critical reading of the manuscript.

References

[1] W.D. Schubert, O. Kuklas, N. Krauss, W. Saenger, P. Fromme, H.T. Witt, Photosystem I of *Synechococcus elongatus* at 4 Å resolution: comprehensive structure analysis, J. Mol. Biol. 274 (1999) 7351–7360.
[2] N. Krauss, W.D. Schubert, O. Klukas, P. Fromme, H.T. Witt, W. Saenger, Photosystem I at 4 Å resolution represents the first structural model of a joint photosynthetic reaction centre and core antenna system, Nat. Struct. Biol. 3 (1996) 965–973.
[3] P. Jordan, P. Fromme, H.T. Witt, O. Klukas, W. Saenger, N. Krauss, Three-dimensional structure of cyanobacterial Photosystem I at 2.5 Å resolution, Nature 411 (2001) 909–917.
[4] B. Kok, On the reversible absorption change at 705 nm in photosynthetic organisms, Biochim. Biophys. Acta 22 (1956) 399–401.
[5] G. Döring, J.R. Bailey, J. Weikara, H.T. Witt, Some new results in photosynthesis, the action of two chlorophyll *a* molecules in light reaction I of photosynthesis, Naturwissenschaften 5 (1968) 219–224.
[6] B. Ke, The rise time of photoreduction, difference spectrum, and oxidation-reduction potential of P430, Arch. Biochem. Biophys. 152 (1972) 70–77.
[7] J. Bonnerjea, M.C.W. Evans, Identification of multiple components in the intermediary electron carrier complex of Photosystem I, FEBS Lett. 148 (1982) 313–316.
[8] P. Gast, T. Swarthoff, F.C.R. Ebskamp, A.J. Hoff, Evidence for a new early acceptor in Photosystem I of plants. An ESR investigation of reaction center triplet yield and of the reduced intermediary acceptors, Biochim. Biophys. Acta 722 (1983) 163–175.
[9] A.M.V. Nuijs, V.A. Shuvalov, H.J. van Gorkom, J.J. Plijter, L.N.M. Duysens, Picosecond absorbance difference spectroscopy on the

primary reactions and the antenna excited states in Photosystem I particles, Biochim. Biophys. Acta 850 (1987) 310–318.
[10] R.W. Mansfield, M.C.W. Evans, UV optical difference spectrum associated with the reduction of electron acceptor A_1 in Photosystem I of higher plants, FEBS Lett. 190 (1985) 237–241.
[11] M.R. Wasiliewsi, J.M. Fenton, Govinjee, The rate of formation of the P_{700}^{+} A_0^{-} in Photosystem I particles from spinach as measured by picosecond transient absorption spectroscopy, Photosynth. Res. 12 (1987) 181–190.
[12] P. Mathis, I. Ikegami, P. Setif, Nanosecond flash studies of the absorption spectrum of the Photosystem I primary acceptor A_0, Photosynth. Res. 16 (1988) 203–210.
[13] V.A. Shuvalov, A.V. Klevanik, A.V. Sharkov, P.G. Kryukov, B. Ke, Picosecond spectroscopy of Photosystem I reaction centers, FEBS Lett. 107 (1979) 313–316.
[14] G. Hastings, F.A. Kleinherenbrink, S. Lin, T.J. McHugh, R.E. Blankenship, Observation of the reduction and reoxidation of the primary electron acceptor in Photosystem I, Biochemistry 33 (1994) 3193–3200.
[15] B. Hecks, K. Wulf, J. Breton, W. Leibl, H.W. Trissl, Primary charge separation in Photosystem I: a two-step electrogenic charge separation connected with P_{700}^{+} A_0^{-} and P_{700}^{+} A_1^{-} formation, Biochemistry 33 (1994) 8619–8624.
[16] S. Kumazaki, M. Iwaki, I. Ikegami, H. Kandori, K. Yoshihara, S. Itoh, Rates of primary electron transfer reactions in the Photosystem I reaction center reconstituted with different quinones as the secondary acceptor, J. Phys. Chem. B 98 (1994) 11220–11225.
[17] S. Savikhin, W. Xu, P.R. Chitnis, W.S. Struve, UltraFAst primary processes in PS I from *Synechocystis* sp. PCC 6803: roles of P_{700} and A_0, Biophys. J. 79 (2000) 1573–1586.
[18] S. Savikhin, W. Xu, P. Martinsson, P.R. Chitnis, W.S. Struve, Kinetics of charge separation and $A_0^{-} > A_1$ electron transfer in Photosystem I reaction centers, Biochemistry 40 (2001) 9282–9290.
[19] K. Brettel, Electron transfer and arrangement of the redox cofactor in Photosystem I, Biochim. Biophys. Acta Bionerg. 1318 (1997) 322–373.
[20] P. Heathcote, P. Moenne-Loccoz, S.E.J. Rigby, M.C.W. Evans, Photoaccumulation in Photosystem I does produce a phylloquinone (A_1^{-}) radical, Biochemistry 35 (1996) 6644–6650.
[21] R.R. Rustandi, S.W. Snyder, L.L. Feezel, T.J. Michalski, J.R. Norris, M.C. Thurnauer, J. Biggins, Contribution of vitamin K_1 to the electron spin polarization in spinach Photosystem I, Biochemistry 29 (1990) 8030–8032.
[22] S.W. Snyder, R.R. Rustandi, J. Biggins, J.R. Norris, M.C. Thurnauer, Direct assignment of vitamin K_1 as the secondary acceptor A_1 in Photosystem I, Proc. Natl. Acad. Sci. U. S. A. 88 (1991) 9895–9896.
[23] K. Brettel, M.H. Vos, Spectroscopic resolution of the picosecond reduction kinetics of the secondary electron acceptor A_1 in Photosystem I, FEBS Lett. 447 (1999) 315–317.
[24] M.C.W. Evans, R. Cammack, The effect of the redox state of the bound iron–suphur centres in spinach chloroplasts on the reversibility of P_{700} photooxidation at low temperatures, Biochem. Biophys. Res. Commun. 63 (1975) 187–193.
[25] M.C.W. Evans, S.G. Reeves, R. Cammack, Determination of the oxidation-reduction potential of the bound iron–sulphur proteins of the primary electron acceptor complex of Photosystem I in spinach chloroplasts, FEBS Lett. 49 (1974) 111–114.
[26] M.C.W. Evans, C.K. Sihra, J.R. Bolton, R. Cammack, Primary electron acceptor complex of Photosystem I in spinach chloroplasts, Nature 256 (1975) 668–670.
[27] M.C. Evans, C.K. Sihra, R. Cammack, The properties of the primary electron acceptor in the Photosystem I reaction centre of spinach chloroplasts and its interaction with P_{700} and the bound ferredoxin in various oxidation-reduction states, Biochem. J. 158 (1976) 71–77.
[28] P. Heathcote, D.L. Williams-Smith, M.C.W. Evans, Quantitative electron-paramagnetic-resonance measurements of the electron-transfer components of the Photosystem-I reaction centre. The reaction-centre chlorophyll (P_{700}), the primary electron acceptor X and bound iron–sulphur centre A, Biochem. J. 170 (1978) 373–378.
[29] D.L. Williams-Smith, P. Heathcote, C.K. Sihra, M.C.W. Evans, Quantitative electron-paramagnetic-resonance measurements of the electron-transfer components of the Photosystem-I reaction centre, Biochem. J. 170 (1978) 365–371.
[30] J.H. Golbeck, B.R. Velthuys, B. Kok, Evidence that the intermediate electron acceptor, A_2, in Photosystem I is a bound iron–sulfur protein, Biochim. Biophys. Acta 504 (1978) 226–230.
[31] J.T. Warden, J.H. Golbeck, Photosystem I charge separation in the absence of centers A and B: II. ESR spectral characterization of center 'X' and correlation with optical signal 'A_2', Biochim. Biophys. Acta 849 (1986) 25–31.
[32] A.E. McDermott, V.K. Yachandra, R.D. Guiles, K. Sauer, M.P. Klein, K.G. Parrett, J.H. Golbeck, EXAFS structural study of F_X, the low-potential Fe–S center in Photosystem I, Biochemistry 28 (1989) 8056–8059.
[33] P. Moenne-Loccoz, P. Heathcote, D.J. Maclachlan, M.C. Berry, I.H. Davis, M.C.W. Evans, Path of electron transfer in Photosystem 1: direct evidence of forward electron transfer from A_1 to Fe–S_x, Biochemistry 33 (1994) 10037–10042.
[34] K. Brettel, J.H. Golbeck, Spectral kinetic characterisation of electron transfer acceptor A_1 in Photosystem I core devoid of iron–sulphur clusters F_X, F_A, and F_B, Photosynth. Res. 45 (1996) 183–193.
[35] K. Brettel, Electron transfer from A_1^{-} to an iron–sulfur center with $t_{1/2}$=200 ns at room temperature in Photosystem I, characterization by flash absorption spectroscopy, FEBS Lett. 239 (1988) 93–98.
[36] P. Joliot, A. Joliot, In vivo analysis of the electron transfer within Photosystem I: are the two phylloquinones involved? Biochemistry 38 (1999) 11130–11136.
[37] M. Guergova-Kuras, B. Boudreaux, A. Joliot, P. Joliot, K. Redding, Evidence for two active branches for electron transfer in Photosystem I, Proc. Natl. Acad. Sci. U. S. A. 98 (2001) 4437–4442.
[38] R. Agalov, K. Brettel, Temperature dependence of biphasic forward electron transfer from the phylloquinone(s) A_1 in Photosystem I: only the slower phase is activated, Biochim. Biophys. Acta Bioenerg. 1604 (2003) 7–12.
[39] V.P. Shinkarev, I.R. Vassiliev, J.H. Golbeck, A kinetic assessment of the sequence of electron transfer from F(X) to F(A) and further to F(B) in Photosystem I: the value of the equilibrium constant between F(X) and F(A), Biophys. J. 78 (2000) 363–372.
[40] P. Heathcote, D.L. Williams-Smith, C.K. Sihra, M.C.W. Evans, The role of the membrane-bound iron–sulphur centres A and B in the Photosystem I reaction centre of spinach chloroplasts, Biochim. Biophys. Acta 503 (1978) 333–342.
[41] J.H. Golbeck, J.T. Warden, Electron spin resonance studies of the bound iron–sulfur centers in Photosystem I. Photoreduction of center A occurs in the absence of center B, Biochim. Biophys. Acta Bioenerg. 681 (1982) 77–84.
[42] H. Oh-oka, Y. Takahaschi, H. Matsubara, S. Itoh, EPR studies of a 9 kDa polypeptide with an iron–sulfur cluster(s) isolated from Photosystem I complex by *n*-butanol extraction, FEBS Lett. 234 (1988) 291–294.
[43] R.M. Wynn, R. Malkin, Characterization of an isolated chloroplast membrane Fe–S protein and its identification as the Photosystem I Fe–S_A/Fe–S_B binding protein, FEBS Lett. 229 (1989) 293–297.
[44] H. Koike, M. Ikeuschi, T. Hiyama, Y. Inoue, Identification of Photosystem I components from the cyanobacterium, *Synechococcus vulcanus* by N-terminal sequencing, FEBS Lett. 253 (1989) 257–263.
[45] P. Setif, Ferredoxin and flavodoxin reduction by Photosystem I, Biochim. Biophys. Acta 1507 (2001) 161–179.
[46] A. Ben-Shem, F. Frolow, N. Nelson, Crystal structure of plant Photosystem I, Nature 426 (2003) 630–635.
[47] K. Brettel, W. Leibl, Electron transfer in Photosystem I, Biochim. Biophys. Acta 1507 (2001) 100–114.

[48] W. Xu, P. Chitnis, A. Valieva, A. van der Est, Y.N. Pushkar, M. Krzystyniak, C. Teutloff, S.G. Zech, R. Bittl, D. Stehlik, B. Zybailov, G. Shen, J.H. Golbeck, Electron transfer in cyanobacterial Photosystem I: I. Physiological and spectroscopic characterization of site-directed mutants in a putative electron transfer pathway from A_0 through A_1 to F_X, J. Biol. Chem. 278 (2003) 27864–27875.

[49] W. Xu, P.R. Chitnis, A. Valieva, A. van der Est, K. Brettel, M. Guergova-Kuras, Y.N. Pushkar, S.G. Zech, D. Stehlik, G. Shen, B. Zybailov, J.H. Golbeck, Electron transfer in cyanobacterial Photosystem I: II. Determination of forward electron transfer rates of site-directed mutants in a putative electron transfer pathway from A_0 through A_1 to F_X, J. Biol. Chem. 278 (2003) 27876–27887.

[50] I.P. Muhiuddin, P. Heathcote, S. Carter, S. Purton, S.E. Rigby, M.C.W. Evans, Evidence from time resolved studies of the P_{700}^{+}/A_1^{-} radical pair for photosynthetic electron transfer on both the PsaA and PsaB branches of the Photosystem I reaction centre, FEBS Lett. 503 (2001) 56–60.

[51] W.V. Fairclough, A. Forsyth, M.C. Evans, S.E. Rigby, S. Purton, P. Heathcote, Bidirectional electron transfer in Photosystem I: electron transfer on the PsaA side is not essential for phototrophic growth in *Chlamydomonas*, Biochim. Biophys. Acta 1606 (2003) 43–55.

[52] R.O. Cohen, G. Shen, J.H. Golbeck, W. Xu, P.R. Chitnis, A.I. Valieva, A. van der Est, Y. Pushkar, D. Stehlik, Evidence for asymmetric electron transfer in cyanobacterial Photosystem I: analysis of a methionine-to-leucine mutation of the ligand to the primary electron acceptor A_0, Biochemistry 43 (2004) 4741–4754.

[53] E. Schlodder, K. Falkenberg, M. Gergeleit, K. Brettel, Temperature dependence of forward and reverse electron transfer from A_1^{-}, the reduced secondary electron acceptor in Photosystem I, Biochemistry 37 (1998) 9466–9476.

[54] M.C. Thurnauer, M.K. Bowman, J.R. Norris, Time-resolved electron spin echo spectroscopy applied to study of photosynthesis, FEBS Lett. 100 (1979) 309–312.

[55] M.C. Thurnauer, J.R. Norris, An electron spin echo phase shift observed in photosynthetic algae. Possible evidence for dynamic radical pair interaction, Chem. Phys. Lett. 76 (1980) 557–561.

[56] C.H. Bock, A.J. van der Est, K. Brettel, D. Stehlik, Nanosecond electron transfer kinetics in Photosystem I as obtained from transient EPR at room temperature, FEBS Lett. 247 (1989) 91–96.

[57] A. van der Est, C. Bock, J. Golbeck, K. Brettel, P. Setif, D. Stehlik, Electron transfer from the acceptor A_1 to the iron–sulfur centers in Photosystem I as studied by transient EPR spectroscopy, Biochemistry 33 (1994) 11789–11797.

[58] S. Purton, D.R. Stevens, I.P. Muhiuddin, M.C.W. Evans, S. Carter, S.E. Rigby, P. Heathcote, Site-directed mutagenesis of PsaA residue W_{693} affects phylloquinone binding and function in the Photosystem I reaction center of *Chlamydomonas reinhardtii*, Biochemistry 40 (2001) 2167–2175.

[59] P. Setif, K. Brettel, Forward electron transfer from phylloquinone A_1 to iron–sulfur centers in spinach Photosystem I, Biochemistry 32 (1993) 7846–7854.

[60] K.M. Salikhov, Y.N. Pushkar, J.H. Golbeck, D. Stehlik, Interpretation of the multifrequency transient EPR spectra of the P_{700}^{+} $A_0QK_1^{-}$ state in Photosystem I particles with a sequential correlated radical pair model: wild type versus A_0 mutants, Appl. Magn. Reson. 24 (2003) 249–259.

[61] S. Santabarbara, I. Kuprov, W.V. Fairclough, S. Purton, P.J. Hore, P. Heathcote, M.C.W. Evans, Bidirectional electron transfer in Photosystem I: determination of two distances between P_{700}^{+} and A_1^{-} in spin-correlated radical pairs, Biochemistry 44 (2005) 2119–2128.

[62] B. Boudreaux, F. MacMillan, C. Teutloff, R. Agalarov, F. Gu, S. Grimaldi, R. Bittl, K. Brettel, K. Redding, Mutations in both sides of the Photosystem I reaction center identify the phylloquinone observed by electron paramagnetic resonance spectroscopy, J. Biol. Chem. 276 (2001) 37299–37306.

[63] P. Setif, K. Brettel, Photosystem I photochemistry under highly reducing conditions: study of the P_{700} triplet state formation from the secondary radical pair (P_{700}^{+} A_1^{-}), Biochim. Biophys. Acta Bioenerg. 1020 (1990) 232–238.

[64] P. Setif, P. Mathis, T. Vänngård, Photosystem I photochemistry at low temperature. Heterogeneity in pathways for electron transfer to the secondary acceptors and for recombination processes, Biochim. Biophys. Acta Bioenerg. 767 (1984) 404–414.

[65] V.A. Shuvalov, The study of the primary photoprocesses in Photosystem I of chloroplasts. Recombination luminescence, chlorophyll triplet state and triplet–triplet annihilation, Biochim. Biophys. Acta 430 (1976) 113–121.

[66] H. Käss, P. Fromme, H.T. Witt, W. Lubitz, Orientation and electronic structure of the primary donor radical cation P_{700}^{+} in Photosystem I: a single crystal EPR and ENDOR study, J. Phys. Chem. B 105 (2001) 1225–1239.

[67] H. Käss, P. Fromme, W. Lubitz, Quadrupole parameters of nitrogen nuclei in the cation radical P_{700}^{+} determined by ESEEM of single crystals of Photosystem I, Chem. Phys. Lett. 257 (1996) 197–206.

[68] L. Krabben, E. Schlodder, R. Jordan, D. Carbonera, G. Giacometti, H. Lee, A.N. Webber, W. Lubitz, Influence of the axial ligands on the spectral properties of P_{700} of Photosystem I: a study of site-directed mutants, Biochemistry 39 (2000) 13012–13025.

[69] A. Petrenko, A.L. Maniero, J. van Tol, F. MacMillan, Y. Li, L.C. Brunel, K. Redding, A high-field EPR study of P_{700}^{+} in wild-type and mutant Photosystem I from *Chlamydomonas reinhardtii*, Biochemistry 43 (2004) 1781–1786.

[70] S.E. Rigby, M.C.W. Evans, P. Heathcote, Electron nuclear double resonance (ENDOR) spectroscopy of radicals in Photosystem I and related Type 1 photosynthetic reaction centres, Biochim. Biophys. Acta 1507 (2001) 247–259.

[71] R. Bittl, S.G. Zech, Pulsed EPR study of spin correlated radical pairs in photosynthetic reaction centres: measurements of the distance between P_{700}^{+} and A_1^{-} in Photosystem I and $P685^{+}$ and Q_A^{-} in bacterial reaction centres, J. Phys. Chem. B 101 (1997) 1429–1436.

[72] B. Guigliarelli, J. Guillaussier, P. Bertrand, J.P. Gayda, P. Setif, Evidence for only one iron–sulfur cluster in center X of Photosystem I from higher plants, J. Biol. Chem. 264 (1989) 6025–6028.

[73] B. Guigliarelli, J. Guillaussier, C. More, P. Setif, H. Bottin, P. Bertrand, Structural organization of the iron–sulfur centers in *Synechocystis* 6803 Photosystem I. EPR study of oriented thylakoid membranes and analysis of the magnetic interactions, J. Biol. Chem. 268 (1993) 900–908.

[74] M.C.W. Evans, P. Heathcote, Effects of glycerol on the redox properties of the electron acceptor complex in spinach Photosystem I particles, Biochim. Biophys. Acta 590 (1980) 89–96.

[75] S.K. Chamorowsky, R. Cammack, Direct determination of the midpoint potential of the acceptor X in chloroplast Photosystem I by electrochemical reduction and electron spin resonance, Photochem. Photobiophys. 4 (1982) 195–200.

[76] K.G. Parrett, T. Mehari, P.G. Warren, J.H. Golbeck, Purification and properties of the intact P_{700}- and Fx-containing Photosystem I core protein, Biochim. Biophys. Acta 973 (1989) 324–332.

[77] B. Ke, W.A. Bulen, E.R. Shaw, R.H. Breeze, Determination of oxidation-reduction potentials by spectropolarimetric titration: application to several iron–sulfur proteins, Arch. Biochem. Biophys. 162 (1974) 301–309.

[78] B. Ke, E. Dolan, K. Sugahara, F.M. Hawkridge, S. Demeter, E. Shaw, Photosynthetic organelles, Plant Cell Physiol. (1977) 187–199 (Special issue).

[79] R. Jordan, U. Nessau, E. Schlodder, Charge recombination between the reduced iron–sulphur centres and $P700^{+}$, in: G. Garab (Ed.), Photosynthesis: Mechanism and Effects, Kluwer Academic Pulisher, Dordrecht, 1998.

[80] M. Iwaki, S. Kumazaki, K. Yoshihara, T. Erabi, S. Itoh, ΔG^0 Dependence of the electron transfer rate in the photosynthetic

reaction center of plant Photosystem I: natural optimization of reaction between chlorophyll *a* (A_0) and quinone, J. Phys. Chem. B 100 (1996) 10802–10809.
[81] S. Itoh, M. Iwaki, I. Ikegami, Modification of Photosystem I reaction center by extraction and exchange of chlorophylls and quinone, Biochim. Biophys. Acta Bioenerg. 1507 (2001) 115–138.
[82] H. Ishikita, E.-W. Knapp, Redox potential of quinones in both electron transfer branches of Photosystem I, J. Biol. Chem. 26 (2003) 2200–52011.
[83] D. Devault, Quantum mechanical tunnelling in biological systems, Q. Rev. Biophys. 13 (1980) 387–564.
[84] R.A. Marcus, N. Sutin, Electron transfer in chemistry and biology, Biochim. Biophys. Acta Bioenerg. 811 (1985) 265–322.
[85] C.C. Moser, P.L. Dutton, Engineering protein structure for electron transfer function in photosynthetic reaction centers, Biochim. Biophys. Acta 1101 (1992) 171–176.
[86] R.A. Marcus, On the theory of oxidation-reduction reactions involving electron transfer, J. Chem. Phys. 24 (1956) 966–978.
[87] R.A. Marcus, On the theory of oxidation-reduction reactions: IV. Unified treatment of homogeneous and electrode reactions, J. Chem. Phys. 43 (1965) 679–701.
[88] R.A. Marcus, B.J. Zwolinski, H. Eyring, The electron tunnelling hypothesis for electron exchange reactions, J. Phys. Chem. 58 (1954) 432–437.
[89] J.J. Hopfield, Electron transfer between biological molecules by thermally activated tunnelling, Proc. Natl. Acad. Sci. U. S. A. 71 (1974) 3640–3644.
[90] C.C. Moser, J.M. Keske, K. Warncke, R.S. Farid, P.L. Dutton, Nature of biological electron transfer, Nature 355 (1992) 796–802.
[91] C.C. Page, C.C. Moser, X. Chen, P.L. Dutton, Natural engineering principles of electron tunnelling in biological oxidation-reduction, Nature 402 (1999) 47–52.
[92] N. Ivashin, S. Larsson, Electron transfer pathways in Photosystem I reaction centers, Chem. Phys. Lett. 275 (2003) 383–387.
[93] B. Munge, S.K. Das, Llagan, Z. Pendon, J. Yang, H.A. Frank, J.F. Rusling, Electron transfer reactions of redox cofactors in spinach Photosystem I reaction centre proteins in lipid films on electrodes, J. Am. Chem. Soc. 125 (2003) 12457–12463.
[94] F.A. Kleinherenbrink, G. Hastings, B.P. Wittmerhaus, R.E. Blankenship, Delayed fluorescence from Fe–S type photosynthetic reaction centers at low redox potential, Biochemistry 33 (1994) 3096–3105.
[95] M.H. Vos, H.J. van Gorkom, Thermodynamics of electron transfer in Photosystem I studied by electric field-stimulated charge recombination, Biochim. Biophys. Acta Bioenerg. 934 (1988) 293–302.
[96] M.H. Vos, H.J. van Gorkom, Thermodynamics and structural information on photosynthetic systems obtained from electroluminescence kinetics, Biophys. J. 58 (1990) 1547–1555.
[97] V.V. Shubin, I.N. Bezsmertnaya, N.V. Karapetyan, Isolation from *Spirulina* membranes of two Photosystem I-type complexes, one of which contains chlorophyll responsible for the 77 K fluorescence band at 760 nm, FEBS Lett. 309 (1992) 340–342.
[98] V.V. Shubin, V.L. Tsuprun, I.N. Bezsmertnaya, N.V. Karapetyan, Trimeric forms of the Photosystem I reaction center complex pre-exist in the membranes of the cyanobacterium *Spirulina platensis*, FEBS Lett. 334 (1993) 79–82.
[99] J. van der Lee, D. Bald, S.L.M. Kwa, R. van Grondelle, M. Rogner, J.P. Dekker, Steady-state polarized-light spectroscopy of isolated Photosystem-I complexes, Photosynth. Res. 35 (1993) 311–321.
[100] L.O. Palsson, J.P. Dekker, E. Schlodder, R. Monshouwer, R. van Grondelle, Polarised site-selected fluorescence spectroscopy of long-wavelength emitting chlorophyll in isolated Photosytem I particles of *Synechococcus elongatus*, Photosynth. Res. 48 (1996) 239–246.
[101] B. Gobets, H. van Amerongen, R. Monshouwer, J. Kruip, M. Rogner, R. van Grondelle, J.P. Dekker, Polarised site-selected fluorescence of isolated Photosystem I, Biochim. Biophys. Acta 1188 (1994) 75–85.
[102] B. Gobets, R. van Grondelle, Energy transfer and trapping in Photosystem I, Biochim. Biophys. Acta 1507 (2001) 80–99.
[103] R. Croce, G. Zucchelli, F.M. Garlaschi, R. Bassi, R.C. Jennings, Excited state equilibration in the Photosystem I-light-harvesting I complex: P_{700} is almost isoenergetic with its antenna, Biochemistry 35 (1996) 8572–8579.
[104] R. Croce, G. Zucchelli, F.M. Garlaschi, R.C. Jennings, A thermal broadening study of the antenna chlorophylls in PS I-200, LHCI, and PS I core, Biochemistry 37 (1998) 17355–17360.
[105] A. Cometta, G. Zucchelli, N.V. Karapetyan, E. Engelmann, F.M. Garlaschi, R.C. Jennings, Thermal behavior of long wavelength absorption transitions in *Spirulina platensis* Photosystem I trimers, Biophys. J. 79 (2000) 3235–3243.
[106] E. Engelmann, T. Tagliabue, N.V. Karapetyan, F.M. Garlaschi, G. Zucchelli, R.C. Jennings, CD spectroscopy provides evidence for excitonic interactions involving red-shifted chlorophyll forms in Photosystem I, FEBS Lett. 499 (2001) 112–115.
[107] B. Gobets, I.H. van Stokkum, M. Rogner, J. Kruip, E. Schlodder, N.V. Karapetyan, J.P. Dekker, R. van Grondelle, Time-resolved fluorescence emission measurements of Photosystem I particles of various cyanobacteria: a unified compartmental model, Biophys. J. 81 (2001) 407–424.
[108] N.V. Karapetyan, Organization and role of the long-wave chlorophylls in the Photosystem I of the cyanobacterium *Spirulina*, Membr. Cell Biol. 12 (1998) 571–584.
[109] V. Zazubovich, S. Matsuzaki, T.W. Johnson, J.M. Hayes, P. Chitnis, G.J. Small, Red antenna states of Photosystem I from the cyanobacterium *Synechococcus elongatus*: a spectral hole burning study, Chem. Phys. 275 (2003) 47–59.
[110] R.C. Jennings, G. Zucchelli, R. Croce, F.M. Garlaschi, The photochemical trapping rate from red spectral states in PS I–LHCI is determined by thermal activation of energy transfer to bulk chlorophylls, Biochim. Biophys. Acta Bioenerg. 1557 (2003) 91–98.
[111] R.C. Jennings, F.M. Garlaschi, E. Engelmann, G. Zucchelli, The room temperature emission band shape of the lowest energy chlorophyll spectral form of LHCI, FEBS Lett. 547 (2003) 107–110.
[112] B. Gobets, J.P. Dekker, R. van Grondelle, Tranfer-to-trap limited model of energy model of energy transfer in PS I, in: G. Garab (Ed.), Photosyntheis: Mechanism and Effects, Kluver academic, Dordrecht, 1998, pp. 503–508.
[113] K. Gibasiewicz, V.M. Ramesh, A.N. Melkozernov, S. Lin, W. Woodbury, R.E. Blankenship, A.N. Webber, Excitation dynamics in the core antenna of PS I from *Chlamydomonas reinhardtii* CC 2696 at room temperature, J. Phys. Chem. B 105 (2001) 11498–11506.
[114] K. Gibasiewicz, A. Dobek, J. Breton, W. Leibl, Modulation of primary radical pair kinetics and energetics in Photosystem II by the redox state of the quinone electron acceptor Q(A), Biophys. J. 80 (2001) 1617–1630.
[115] B. Gobets, I.H. van Stokkum, F. van Mourik, J.P. Dekker, R. van Grondelle, Excitation wavelength dependence of the fluorescence kinetics in Photosystem I particles from *Synechocystis* PCC 6803 and *Synechococcus elongatus*, Biophys. J. 85 (2003) 3883–3898.
[116] K. Gibasiewicz, V.M. Ramesh, S. Lin, W. Woodbury, A.N. Webber, Excitation dynamics in eukaryotic PS I from *Chlamydomonas reinhardtii* CC 2696 at 10 K. Direct detection of the reaction centres states, J. Phys. Chem. B 106 (2002) 6322–6330.
[117] M. Du, X.L. Xie, Y.W. Jia, L. Mets, G.R. Fleming, Direct observation of ultrafast energy transfer in PS I core antenna, Chem. Phys. Lett. 201 (1993) 535–542.
[118] R. Croce, D. Dorra, A.R. Holzwarth, R.C. Jennings, Fluorescence decay and spectral evolution in intact Photosystem I of higher plants, Biochemistry 39 (2000) 6341–6348.
[119] R.J. Gulotty, L. Mets, R.S. Alberte, G.R. Fleming, Picosecond fluorescence study of photosynthetic mutants of *Chlamydomonas reinhardii*: origin of the fluorescence decay kinetics of chloroplasts, Photochem. Photobiol. 41 (1985) 487–496.
[120] G. Hastings, F.A.M. Kleinherenbrink, S. Lin, R.E. Blankenship, Time resolved fluorescence and absorption spectroscopy of Photosystem I, Biochemistry 33 (1994) 3185–3192.

[121] S. Kumazaki, H. Kandori, H. Petek, K. Yoshihara, I. Ikegami, Primary photochemical processes in P700-enriched Photosystem I particles: trap-limited excitation decay and primary charge separation, J. Phys. Chem. B 98 (1994) 10335–10342.
[122] N.T.G. White, G.S. Beddard, J.R.G. Thorne, T.M. Feehan, T.E. Keyes, P. Heathcote, Primary charge separation and energy transfer in Photosystem I reaction centre of higher plants, J. Phys. Chem. B 100 (1996) 12086–12099.
[123] J.T.M. Kennis, B. Gobets, I.H.M. van Stokkum, J.P. Dekker, R. van Grondelle, G.R. Fleming, Light harvesting by chlorophylls and carotenoids in the Photosystem I core complex of *Synechococcus elongatus*: a fluorescence upconversion study, J. Phys. Chem. B 105 (2001) 1194–4485.
[124] A.N. Melkozernov, Excitation energy transfer in Photosystem I from oxygenic organism, Photosynth. Res. 70 (2001) 129–153.
[125] A.N. Melkozernov, J. Kargul, S. Lin, J. Barber, R.E. Blankenship, Energy coupling in the PS I–LHCI supercomplex from the green alga *Chlamydomonas reinhardtii*, J. Phys. Chem. B 108 (2004) 10547–10555.
[126] A.N. Melkozernov, S. Lin, R.E. Blankenship, Femtosecond transient spectroscopy and excitonic interaction in Photosystem I, J. Phys. Chem. B 104 (2000) 1615–1656.
[127] A.N. Melkozernov, S. Lin, R.E. Blankenship, Femtosecond transient spectroscopy and excitonic interactions in Photosystem I, J. Phys. Chem. B 104 (2000) 1651–1656.
[128] A.N. Melkozernov, S. Lin, R.E. Blankenship, Excitation dynamics and heterogeneity of energy equilibration in the core antenna of Photosystem I from the cyanobacterium *Synechocystis* sp. PCC 6803, Biochemistry 39 (2000) 1489–1498.
[129] A.N. Melkozernov, S. Lin, V.H. Schmid, H. Paulsen, G.W. Schmidt, R.E. Blankenship, Ultrafast excitation dynamics of low energy pigments in reconstituted peripheral light-harvesting complexes of Photosystem I, FEBS Lett. 471 (2000) 89–92.
[130] M.G. Muller, J. Niklas, W. Lubitz, A.R. Holzwarth, Ultrafast transient absorption studies on Photosystem I reaction centers from *Chlamydomonas reinhardtii*: 1. A new interpretation of the energy trapping and early electron transfer steps in Photosystem I, Biophys. J. 85 (2003) 3899–3922.
[131] T.G. Owens, S.P. Webb, L. Mets, R.S. Alberte, G.R. Fleming, Antenna size dependence of fluorescence decay in the core antenna of Photosystem I: estimates of charge separation and energy transfer rates, Proc. Natl. Acad. Sci. U. S. A. 84 (1987) 1532–1536.
[132] T.G. Owens, S.P. Webb, L. Mets, R.S. Alberte, G.R. Fleming, Antenna structure and excitation dynamics in Photosystem I: II. Studies with mutants of *Chlamydomonas reinhardtii* lacking photosystem, Biophys. J. 56 (1989) 95–106.
[133] L.O. Palsson, C. Flemming, B. Gobets, R. van Grondelle, J.P. Dekker, E. Schlodder, Energy transfer and charge separation in Photosystem I: P_{700} oxidation upon selective excitation of the long-wavelength antenna chlorophylls of *Synechococcus elongatus*, Biophys. J. 74 (1998) 2611–2622.
[134] S. Turconi, J. Kruip, G. Schweitzer, M. Rogner, A.R. Holzwarth, A comparative fluorescence kinetic study of Photosystem I monomers and trimers from *Synechocystis* PCC 6803, Photosynth. Res. 49 (1996) 263–268.
[135] S. Turconi, G. Schweitzer, A.R. Holzwarth, Temperature dependence of picosecond fluorescence kinetic of a cyanobacterial Photosystem I particle, Photochem. Photobiol. 57 (1993) 113–119.
[136] S. Savikhin, W. Xu, V. Soukoulis, P.R. Chitnis, W.S. Struve, Ultrafast primary processes in Photosystem I of the cyanobacterium *Synechocystis* sp. PCC 6803, Biophys. J. 76 (1999) 3278–3288.
[137] S. Kumazaki, I. Ikegami, H. Furusawa, S. Yasuda, Yoshihara, Observation of the excited state of the primary electron donor chlorophyll (P_{700}) and the ultrafast charge separation in the spinach Photosystem I reaction centre, Phys. Chem. B. 105 (2001) 1093–1099.
[138] J.M. Fenton, M.J. Pellin, Govinjee, J. Kaufmann, Primary photochemistry of the reaction center of Photosystem I, FEBS Lett. 100 (1979) 1–4.
[139] V.A. Shuvalov, K.E. Bacon, E. Dolan, Kinetic and spectral properties of the intermediary electron acceptor A_1 in Photosystem I. Subnanosecond spectroscopy, FEBS Lett. 100 (1979) 5–8.
[140] V.M. Ramesh, K. Gibasiewicz, S. Lin, S.E. Bingham, A.N. Webber, Bidirectional electron transfer in Photosystem I: accumulation of A_0^- in A-side or B-side mutants of the axial ligand to chlorophyll A_0, Biochemistry 43 (2004) 1369–1375.
[141] A. Diaz-Quintana, W. Leibl, H. Bottin, P. Setif, Electron transfer in Photosystem I reaction centers follows a linear pathway in which iron–sulfur cluster F_B is the immediate electron donor to soluble ferredoxin, Biochemistry 37 (1998) 3429–3439.
[142] G.S. Beddard, Exciton coupling in Photosystem I reaction centres, J. Phys. Chem. B 102 (1998) 10966–10973.
[143] G.S. Beddard, Excitations and excitons in Photosystem I, Philos. Trans. R. Soc. Lond., A 356 (1998) 421–448.
[144] H.J. den Blanken, A.J. Hoff, High-resolution absorbance-difference spectra of the triplet state of the primary donor P_{700} in Photosystem I subchloroplast particles measured with absorbance-detected magnetic resonance at 1.2 K. Evidence that P_{700} is a dimeric chlorophyll complex, Biochim. Biophys. Acta 724 (1983) 52–61.
[145] D. Carbonera, P. Collareta, G. Giacometti, The P_{700} triplet state in an intact environment detected by ODMR A well resolved triplet minus singlet spectrum, Biochim. Biophys. Acta 1322 (1997) 115–128.
[146] D.E. Budil, M.C. Thurnauer, The chlorophyll triplet state as a probe of structure and function in photosynthesis, Biochim. Biophys. Acta 1057 (1991) 1–41.
[147] G.F.W. Searle, T.J. Schaafsma, Fluorescence detected magnetic resonance of the primary donor and inner core antenna chlorophyll in Photosystem I reaction centre protein: sign inversion and energy transfer, Photosynth. Res. 32 (1992) 193–206.
[148] J. Vrieze, P. Gast, A.J. Hoff, Structure of the reaction center of Photosystem I of plants. An investigation with linear-dichroic absorbance-detected magnetic resonance, J. Phys. Chem. B 100 (1996) 9960–9967.
[149] T. Renger, E. Schlodder, Modeling the optical spectra and light harvesting in Photosystem I, in: J. Golbeck (Ed.), Photosystem I: The Plastocyanin: Ferredoxin Oxidoreductase in Photosynthesis, in press.
[150] Y. Shibata, T. Kasahara, S. Akai, S. Itoh, I. Ikegami. The energy gap between P_{700}^+ A_0^- and P700* in Photosystem I determined by delayed fluorescence at 270–77 K, in: R. Carpentier, D. Bruce, A. van der Est (Eds.), in press.
[151] R.M. Pearlstein, Chlorophyll singlet excitons, in: D. Govindjee (Ed.), Photosynthesis: Energy conversion by Plant and Bacteria, Academic Press, New York, 1982, pp. 294–330.
[152] R.M. Pearlstein, Exciton migration and trapping in photosynthesis, Photochem. Photobiol. 35 (1982) 835–844.
[153] T. Renger, A.R. Marcus, Photophysical properties of PS-2 reaction centers and a discrepancy in exciton relaxation times, J. Phys. Chem. B 106 (2002) 1809–1819.
[154] S.E.J. Rigby, I.P. Muhiuddin, S. Santabarbara, M.C.W. Evans, P. Heathcote, Proton ENDOR spectroscopy of the anion radicals of the chlorophyll primary electron acceptor in type I photosynthetic reaction centres, Chem. Phys. 294 (2003) 319–328.
[155] P. Heathcote, J.A. Hanley, M.C.W. Evans, Double-reduction of A1 abolishes the EPR signal attributed to A_1: evidence for C2 symmetry in the Photosystem I reaction centre, Biochim. Biochim. Biophys. Acta 1144 (1993) 54–61.
[156] A.N. Webber, W. Lubitz, P_{700}: the primary electron donor of Photosystem I, Biochim. Biophys. Acta 1507 (2001) 61–79.
[157] K. Brettel, in: G. Garab (Ed.), Photosynthesis: Mechanism and Effect, Kluwer Academic Publisher, Dordrecht, 1998, pp. 611–614.
[158] R. Cammack, M.C.W. Evans, E.P.R. spectra of iron–sulphur proteins in dimethylsulphoxide solutions: evidence that chloroplast Photo-

system I particles contain 4Fe–4S centres, Biochem. Biophys. Res. Commun. 67 (1975) 544–549.
[159] H.W. Trissl, P. Graber, II. Electrical measurements in the nanosecond range of the charge separation from chloroplasts spread at a heptane–water interface. Application of a novel capacitive electrode, Biochim. Biophys. Acta 595 (1980) 96–108.
[160] V.P. Shinkarev, B. Zybailov, I.R. Vassiliev, J.H. Golbeck, Modelling of the P^{+}_{700} charge recombination kinetics with phylloquinone and plastoquinone-9 in the A_1 site of Photosystem I, Biophys. J. 83 (2002) 2885–2897.
[161] J.T. Warden, J.H. Golbeck, Electron-spin resonance studies of the bound iron–sulfur centers in Photosystem I: II. Correlation of P_{700} triplet production with urea/ferricyanide inactivation of the iron–sulfur clusters, Biochim. Biophys. Acta 891 (1987) 286–292.
[162] K. Sigfridsson, O. Hansson, P. Brzezinski, Electrogenic light reactions in Photosystem I: resolution of electron-transfer rates between the iron–sulfur centers, Proc. Natl. Acad. Sci. U. S. A. 92 (1995) 3458–3462.
[163] G. Shen, M.L. Antonkine, A. van der Est, I.R. Vassiliev, K. Brettel, R. Bittl, S.G. Zech, J. Zhao, D. Stehlik, D.A. Bryant, J.H. Golbeck, Assembly of Photosystem I: II. Rubredoxin is required for the in vivo assembly of F(X) in *Synechococcus* sp. PCC 7002 as shown by optical and EPR spectroscopy, J. Biol. Chem. 277 (2002) 20355–20366.
[164] A.Y. Semenov, M.D. Mamedov, S.K. Chamorowsky, Photoelectric studies of the transmembrane charge transfer reactions in Photosystem I pigment protein complexes, FEBS Lett. 533 (2003) 223–228.
[165] M.D. Mamedov, K.N. Gourovskaya, I.R. Vassiliev, J.H. Golbeck, A. Sememov, Electrogenicity accompanies photoreduction of the iron–sulfur clusters F(A) and F(B) in Photosystem I, FEBS Lett. 431 (1998) 219–223.
[166] A.A. Mamedova, M.D. Mamedov, K.N. Gourovskaya, I.R. Vassiliev, J.H. Golbeck, A.Y. Semenov, Electrometrical study of electron transfer from the terminal F_A/F_B iron–sulfur clusters to external acceptors in Photosystem I, FEBS Lett. 462 (1999) 421–424.
[167] I.R. Vassiliev, Y.S. Jung, F. Yang, J.H. Golbeck, PsaC subunit of Photosystem I is oriented with iron–sulfur cluster F(B) as the immediate electron donor to ferredoxin and flavodoxin, Biophys. J. 74 (1998) 2029–2035.
[168] I.R. Vassiliev, M.L. Antonkine, J.H. Golbeck, Iron–sulfur clusters in type I reaction centers, Biochim. Biophys. Acta 1507 (2001) 139–160.
[169] J.H. Nugent, B.L. Moller, M.C.W. Evans, Comparison of the EPR properties of Photosystem I iron–sulphur centres A and B in spinach and barley, Biochim. Biophys. Acta 634 (1981) 249–255.
[170] M.T. Zeng, X.M. Gong, M.C. Evans, N. Nelson, C. Carmeli, Stabilization of iron–sulfur cluster F(X) by intra-subunit interactions unraveled by suppressor and second site-directed mutations in PsaB of Photosystem I, Biochim. Biophys. Acta 1556 (2002) 254–264.
[171] A. Van Der Est, A.I. Valieva, Y.E. Kandrashkin, G. Shen, D.A. Bryant, J.H. Golbeck, Removal of PsaF alters forward electron transfer in Photosystem I: evidence for fast reoxidation of QK(A) in subunit deletion mutants of *Synechococcus* sp. PCC 7002, Biochemistry 43 (2004) 1264–1275.
[172] J.R. Alcala, The effect of harmonic conformational trajectories on protein fluorescence and lifetime distributions, J. Phys. Chem. B 101 (1994) 4578–4584.
[173] J.R. Alcala, E. Gratton, F.G. Predergast, Interpretation of fluorescence decays in protein using continuous lifetime distributions, Biophys. J. 51 (1987) 925–936.
[174] J.R. Lakowics, On spectral relaxation in proteins, Photochem. Photobiol. 72 (2000) 421–437.
[175] J.M. Beechem, E. Gratton, M. Ameloot, J.R. Knutson, L. Brand, The Global Analysis of fluorescence intensity and anisotropy decay data: second-generation theory and programs, in: J.R. Lakowicz (Ed.), Topics in Fluoresecnce Spectroscopy, Plenum Press, New York, 1991–1994, pp. 241–301.
[176] M. Straume, S.G. Frasier-Cadoret, M.L. Johnson, Least-squares analysis of fluorescence data, in: J.R. Lakowicz (Ed.), Topics in Fluorescence Spectroscopy, Plenum Press, New York, 1991–1994, pp. 177–239.
[177] A. Ogrodnik, W. Keupp, M. Volk, G. Aumeier, M.-B.M.E., Inhomogeneity of radical pair energies in photosynthetic reaction centers revealed by differences in recombination dynamics of $P^{+}H_A^{-}$ when detected in delayed emission and in absorption, J. Phys. Chem. B 98 (1994) 3432–3439.
[178] H.T. Witt, Energy conversion in the functional membranes of photosynthesis. Analysis by light pulse and electric pulse methods. The central role of the electric field, Biochim. Biophys. Acta 505 (1979) 355–427.
[179] W. Junge, H.T. Witt, On the ion transport system of photosynthesis—investigations on a molecular level, Z. Naturforsch. 23b (1968) 244–254.
[180] H.M. Emrich, W. Junge, H.T. Witt, Further evidence for an optical response of chloroplast bulk pigments to a light induced electrical field in photosynthesis, Z. Naturforsch. 24b (1969) 1144–1146.
[181] S. Scmidt, R. Reich, H.T. Witt, in: A. Avron, G. Forti (Eds.), Proc. 2nd. Intern. Conger. Photosynthesis, Stresa, 1972, pp. 1087–1093.
[182] A. Warshel, S.T. Russel, Calculations of electrostatic interactions in biological systems and in solutions, Q. Rev. Biophys. 17 (1984) 283–422.
[183] A. Warshel, W.W. Parson, Computer simulations of electron-transfer reactions in solution and in photosynthetic reaction centers, Annu. Rev. Phys. Chem. 42 (1991) 279–309.
[184] S.E. Rigby, I.P. Muhiuddin, M.C. Evans, S. Purton, P. Heathcote, Photoaccumulation of the PsaB phyllosemiquinone in Photosystem I of *Chlamydomonas reinhardtii*, Biochim. Biophys. Acta 1556 (2002) 13–20.
[185] S.E. Rigby, M.C. Evans, P. Heathcote, ENDOR and special triple resonance spectroscopy of $A_1^{\cdot -}$ of Photosystem 1, Biochemistry 35 (1996) 6651–6656.
[186] P.Q. Setif, H. Bottin, Laser flash absorption spectroscopy study of ferredoxin reduction by Photosystem I in *Synechocystis* sp. PCC 6803: evidence for submicrosecond and microsecond kinetics, Biochemistry 33 (1994) 8495–8504.
[187] P.Q. Setif, H. Bottin, Laser flash absorption spectroscopy study of ferredoxin reduction by Photosystem I: spectral and kinetic evidence for the existence of several Photosystem I–ferredoxin complexes, Biochemistry 34 (1995) 9059–9070.
[188] M.L. Antonkine, D. Bentrop, I. Bertini, C. Luchinat, G. Shen, D.A. Bryant, D. Stehlik, J.H. Golbeck, Paramagnetic 1H NMR spectroscopy of the reduced, unbound Photosystem I subunit PsaC: sequence-specific assignment of contact-shifted resonances and identification of mixed- and equal-valence Fe–Fe pairs in [4Fe–4S] centers F_A and F_B, J. Biol. Inorg. Chem. 5 (2000) 381–392.
[189] D. Bentrop, I. Bertini, C. Luchinat, W. Nietschke, U. Mulenhoff, Characterisation of the unbound 2 [4Fe–4S] ferredoxin-like Photosystem I subunit from the cyanobacterium *Synechococcus elongatus*, Biochemistry 36 (1997) 13629–13637.
[190] R. Kummerle, J. Gaillard, P. Kyritis, J.-M. Moulis, Intramolecular electron transfer in [4Fe–4S] proteins: estimates of the reorgansiation energy and electronic coupling in *Chromatium vinosum* ferredoxin, J. Biol. Inorg. Chem. 6 (2001) 446–451.
[191] P. Kyritsis, J.G. Huber, I. Quinkal, J. Gaillard, J.M. Moulis, Intramolecular electron transfer between [4Fe–4S] cluster studied by proton magnetic resonance spectroscopy, Biochemistry 36 (1997) 7829–7846.
[192] E. Sigfridsson, M.H.M. Olsson, U. Ryde, A comparison of the inner-sphere reorganisation energies of cytochromes, iron–sulphur clusters, and blue copper proteins, J. Phys. Chem. B 105 (2001) 5546–5552.

[193] P. Setif, N. Fischer, B. Lagoutte, H. Bottin, J.D. Rochaix, The ferredoxin docking site of Photosystem I, Biochim. Biophys. Acta Bioenerg. 1555 (2002) 204–209.
[194] W. Leibl, B. Tourpance, J. Breton, Photoelectric characterisation of forward electron transfer to iron–sulphur centres in Photosystem I, Biochemistry 34 (1995) 10237–10244.
[195] A. van der Est, Light-induced spin polarisation in type I reaction centres, Biochim. Biophys. Acta Bioenerg. 1501 (2001) 212–225.
[196] H. Witt, E. Bordignon, D. Carbonera, J.P. Dekker, N. Karapetyan, C. Teutloff, A. Webber, W. Lubitz, E. Schlodder, Species-specific differences of the spectroscopic properties of P_{700}: analysis of the influence of non-conserved amino acid residues by site-directed mutagenesis of Photosystem I from *Chlamydomonas reinhardtii*, J. Biol. Chem. 278 (2003) 46760–46771.
[197] L.N.M. Duysens, The path of light in photosynthesis, The Photochemical Apparatus; Its Structure and Function, Brookhaven National Laboratory, Upton, NY, 1959, pp. 10–25.
[198] R.S. Knox, Thermodynamics and the primary process of photosynthesis, Biophys. J. 9 (1969) 1351–1362.
[199] R.T. Ross, M. Calvin, Thermodynamics of light emission and free-energy storage in photosynthesis, Biophys. J. 7 (1967) 595–614.
[200] J. Lavergne, P. Joliot, Dissipation in bioenergetic transfer chains, Photosynth. Res. 48 (1966) 127–138.
[201] W. Yourgrau, A. van der Merwe, Entropy balance in photosynthesis, Proc. Natl. Acad. Sci. U.S.A. 59 (1968) 734–737.
[202] W.W. Parson, Thermodynamics of the primary reactions of photosynthesis, Photochem. Photobiol. 28 (1978) 389–393.